

# Geochronology of late Albian–Cenomanian strata in the U.S. Western Interior

Brad S. Singer<sup>1,†</sup>, Brian R. Jicha<sup>1</sup>, David Sawyer<sup>2</sup>, Ireneusz Walaszczyk<sup>3</sup>, Robert Buchwaldt<sup>4</sup>, and Jorg Mutterlose<sup>5</sup>

<sup>1</sup>Department of Geoscience, University of Wisconsin–Madison, 1215 West Dayton Street, Madison, Wisconsin 53706, USA

<sup>2</sup>University of Colorado, Boulder; mail address: 955 Adams Street, Denver, Colorado 80206, USA

<sup>3</sup>Faculty of Geology, University of Warsaw, Al. Zwirki i Wigury 92, PL-02-089, Warszawa, Poland

<sup>4</sup>Department of Earth and Environment, Boston University, 685 Commonwealth Avenue, Boston, Massachusetts 02215, USA

<sup>5</sup>Ruhr-Universität Bochum, Institute of Geology, Mineralogy and Geophysics, Universitätsstr. 150, 44780 Bochum, Germany

## ABSTRACT

Since the publication of  $^{40}\text{Ar}/^{39}\text{Ar}$  dates from Cretaceous bentonites in the Western Interior Basin by J.D. Obradovich in 1993 and in Japan by J.D. Obradovich and colleagues in 2002, improvements in the  $^{40}\text{Ar}/^{39}\text{Ar}$  method have included a shift to astronomically calibrated ages for standard minerals and development of a new generation of multi-collector mass spectrometers. Thus, the  $^{40}\text{Ar}/^{39}\text{Ar}$  chronometer can yield results that are synchronous with U-Pb zircon dates and astrochronologic age models for Cretaceous strata. Ages determined by Obradovich have  $\pm 2\sigma$  analytical uncertainties of  $\pm 400$  ka (excluding  $J$  value or systematic contributions) that have been used to discriminate stratigraphic events at ca. 1 Ma resolution. From among several dozen sanidine samples, 32 of which were dated by Obradovich in 1993, we present new multi-collector  $^{40}\text{Ar}/^{39}\text{Ar}$  ages that reduce the average analytical uncertainties by nearly an order of magnitude. These new ages (where the uncertainties also include the contribution of the neutron fluence  $J$  value) include:

- Topmost Bentonite, Mowry Shale, Kaycee, Wyoming, USA,  $97.52 \pm 0.09$  Ma
- Clay Spur Bentonite, Mowry Shale, Casper, Wyoming,  $98.17 \pm 0.11$  Ma
- Arrow Creek Bentonite, Colorado Shale, Montana, USA,  $99.12 \pm 0.14$  Ma
- Upper Newcastle Sandstone, Black Hills, Wyoming,  $99.49 \pm 0.07$  Ma
- Middle Newcastle Sandstone, Black Hills, Wyoming,  $99.58 \pm 0.12$  Ma
- Shell Creek Shale, Bighorn Basin, Crow Reservation, Wyoming,  $99.62 \pm 0.07$  Ma

<sup>†</sup>bsinger@wisc.edu

- Shell Creek Shale, Bighorn Basin, Greybull, Wyoming,  $99.67 \pm 0.13$  Ma
- Shell Creek Shale, Bighorn Basin, Lander, Montana,  $100.07 \pm 0.07$  Ma
- Muddy Sandstone, Wind River Basin, Wyoming,  $101.23 \pm 0.09$  Ma
- Thermopolis Shale, Bighorn Basin, Wyoming,  $101.36 \pm 0.11$  Ma
- Vaughn Member, Blackleaf Formation, Sweetgrass Arch, Montana,  $102.68 \pm 0.07$  Ma
- Taft Hill Member, Blackleaf Formation, Sweetgrass Arch, Montana,  $103.08 \pm 0.11$  Ma
- Base of the Skull Creek Shale, Black Hills, Wyoming,  $104.87 \pm 0.10$  Ma
- Thermopolis Shale, Bighorn Basin, Wyoming,  $106.37 \pm 0.11$  Ma

A new U-Pb zircon age of  $104.69 \pm 0.07$  Ma from the Skull Creek Shale at Dinosaur Ridge, Colorado, USA, is close to the new  $^{40}\text{Ar}/^{39}\text{Ar}$  age of the Skull Creek Shale in the Black Hills, Wyoming, but 5 m.y. is missing in the unconformity between the Skull Creek Shale of the Black Hills and the overlying Newcastle Sandstone. Considering the average total uncertainties that include decay constant and standard age or tracer composition for the  $^{40}\text{Ar}/^{39}\text{Ar}$  ( $\pm 0.19$  Ma) and the U-Pb ( $\pm 0.13$  Ma) ages does not alter this finding. Moreover, the lower Thermopolis Shale in the Bighorn Basin is 1.5 Ma older than the Skull Creek Shale in the Black Hills. The  $100.07 \pm 0.07$  Ma Shell Creek Bentonite in Montana is close to the Albian–Cenomanian boundary age of  $100.2 \pm 0.2$  Ma of Obradovich and colleagues from Hokkaido, Japan, and  $100.5 \pm 0.5$  Ma adopted in the 2012 geological time scale of J.G. Ogg and L.A. Hinnov. Our findings indicate that correlations based on similarity of lithology, without independent radioisotopic ages or detailed bio-

stratigraphic constraints, can be problematic or invalid. There is much more time missing in unconformities than has been previously recognized in these important, petroleum-bearing reservoir strata.

## INTRODUCTION

Upper Cretaceous rocks in the Western Interior Seaway of western North America (USA and Canada) are among the most thoroughly studied sedimentary successions in the Phanerozoic rock record. The paleontology of ammonite and inoceramid molluscs records a detailed pattern of evolutionary radiation, adaptation, and extinction during the highest stands of sea-level across the North American continental interior over more than 25 Ma of Late Cretaceous earth history. This pattern of biologic evolution and lithologic succession is well-constrained by biostratigraphy (Cobban, 1993; Kauffman et al., 1993; Cobban et al., 2006) and radioisotopic geochronology (Obradovich, 1993) based upon ages determined for dozens of bentonite ash layers that are interlayered with marine sedimentary deposits of the Western Interior Seaway. The detailed biostratigraphic and geochronologic framework is the legacy of the distinguished scientific careers of paleontologist Bill Cobban (1916–2015) and geochronologist John Obradovich (1929–2012), who developed a productive collaboration over 30 years while working together for the U.S. Geological Survey in Colorado, USA. Obradovich's pursuit of “putting numerical ages on fossils” coincided with Cobban's zeal for collecting and identifying as many fossils as possible to create a vertically detailed, areally extensive, biostratigraphic framework for the Rocky Mountains and Great Plains (Obradovich and Cobban, 1975; Obradovich, 1993; Cobban et al., 2006).

The advent of  $^{40}\text{Ar}/^{39}\text{Ar}$  laser fusion dating of sanidine by 1990 substantially improved

the precision and accuracy of ages determined using the K-Ar radioisotopic chronometer. The Cretaceous time scale of Obradovich (1993), supplemented by additional ages and magnetostratigraphy for the Campanian-lower Maastrichtian interval by Hicks et al. (1999), provided a high-resolution, geochronologically calibrated ammonite zone biostratigraphy from 96 Ma to 69 Ma. This scheme is based upon 26 bentonite-dated ammonite zones, for an average interpolated ammonite zone duration of 393 ka, consistent with the average analytical uncertainties of  $\pm 400$  ka ( $2\sigma$ ) for the age determinations in Obradovich (1993). The bottom of the Upper Cretaceous was constrained from strata in Hokkaido, Japan, that provided ages of ca. 100 Ma for the Albian–Cenomanian boundary (Obradovich et al., 2002) and the top in Wyoming and Montana, USA, yielding an age of 66 Ma for the Cretaceous–Paleogene boundary (Hicks et al., 2002), which has been confirmed by subsequent radioisotopic dating (Renne et al., 2013; Clyde et al., 2016; Sprain et al., 2018).

In 2008, Obradovich and Cobban supported a re-investigation of the Upper Cretaceous age stratigraphic framework at the University of Wisconsin–Madison, USA, WiscAr Laboratory. They provided access to their archives of stratigraphic information including field notes, purified sanidine samples, and  $^{40}\text{Ar}/^{39}\text{Ar}$  isotopic data in paper form, much of which have not been published. A new set of  $^{40}\text{Ar}/^{39}\text{Ar}$  sanidine dates was determined for many of the key bentonites using higher-precision analytical methods but mostly relying on a type of single-collector mass spectrometer similar to the one used by Obradovich at the U.S. Geological Survey in Menlo Park, California, USA. Generally, this was accomplished by generating a larger number of dates per sample (typically  $n = 6$ –7 for Obradovich versus  $n = 30$ –40 at WiscAr Laboratory). The  $^{40}\text{Ar}/^{39}\text{Ar}$  dates were cross-calibrated against single-zircon U-Pb dates determined by isotope dilution-thermal ionization mass spectrometry (ID-TIMS) at the British Geological Survey in Keyworth, UK, from bentonites at the same localities sampled by Cobban and analyzed by Obradovich (1993). The results were used to integrate  $^{40}\text{Ar}/^{39}\text{Ar}$ , U-Pb, and astronomical clocks and thus establish a new age model for 10 Ma of deposition spanning the Turonian–Coniacian, Coniacian–Santonian, and Santonian–Campanian stage boundaries (Meyers et al., 2012; Sageman et al., 2014). Another finding is that the U-Pb zircon and  $^{40}\text{Ar}/^{39}\text{Ar}$  sanidine dates are brought into close agreement by using the Kuiper et al. (2008) age of  $28.201 \pm 0.046$  Ma for the Fish Canyon sanidine (FCs) standard, thereby supporting the astronomical calibration of this important standard

material. At the same time, Joo and Sageman (2014) published the first continuous carbon and oxygen-isotope bulk-rock record for the Upper Cretaceous (middle Cenomanian–lower Campanian) Western Interior Seaway ammonite biostratigraphic succession. Using these chemoisotopic correlations with the revised  $^{40}\text{Ar}/^{39}\text{Ar}$  ages and independent astrochronologic age models, new ages were proposed for several Upper Cretaceous stage boundaries (Sageman et al., 2014).

More recently, a multi-collector mass spectrometer fitted with four ion-counting electron multipliers deployed in the WiscAr Laboratory, in most cases, can produce  $^{40}\text{Ar}/^{39}\text{Ar}$  dates with a significant improvement in precision compared to those obtained using a single-collector mass spectrometer (e.g., Jicha et al., 2016; Andersen et al., 2017). Multi-collector mass spectrometers have more stable electronics and commonly have exceptionally low hydrocarbon background levels (e.g., Schaen et al., 2020), both of which can result in  $^{40}\text{Ar}/^{39}\text{Ar}$  dates for single Cretaceous sanidine crystals with analytical uncertainties of less than  $\pm 100$  ka (Jicha et al., 2016; Leslie et al., 2018). Thus, a small population of dates can have resulting weighted mean depositional ages with analytical uncertainties of  $\pm 30$ –50 ka, i.e., better than 0.5 per mil. Thus, the multi-collector mass spectrometer is poised to improve upon the precision and accuracy of the legacy data in Obradovich (1993) and Hicks et al. (1999, 2002) by an order of magnitude.

Our aim is to improve on the chronostratigraphy and correlation of problematic, unconformity-bounded sequences of late Albian–early Cenomanian strata of the Western Interior. We present new radioisotopic age determinations from bentonites spanning a ca. 10 Ma interval from 107 Ma to 97 Ma in which temporal constraints are minimal at present. These include  $^{40}\text{Ar}/^{39}\text{Ar}$  measurements of sanidine from six bentonites first dated by Obradovich (1993). Moreover, we report eight new  $^{40}\text{Ar}/^{39}\text{Ar}$  dates from sanidine in bentonites from the late Albian–early Cenomanian interval at the base of the Cretaceous Western Interior sequence that have been correlated with great uncertainties in regard to lithostratigraphic and temporal relations. Two new  $^{40}\text{Ar}/^{39}\text{Ar}$  dates are from the Aptian in Germany and Albian in British Columbia, Canada. These new dates are calibrated relative to the astronomical age of  $28.201 \pm 0.046$  Ma for the FCs standard of Kuiper et al. (2008) that was adopted in the 2012 Geological Time Scale (GTS, 2012; Gradstein et al., 2012). The reasoning for calibrating new and legacy ages to 28.201 Ma FCs is summarized by Schmitz (2012) in GTS 2012, and we have done so using the Java-based ArAR recalibration program of

Mercer and Hodges (2016). We also report three new U-Pb dates from bentonites in the Dakota Sandstone in Colorado. These new radioisotopic dates are the basis of a new age model on which the biostratigraphy and sedimentology of these strata may be correlated and interpreted (e.g., Weimer, 1984, 1996).

## LATE ALBIAN–EARLY CENOMANIAN BOUNDARY INTERVAL

### Stratigraphy

Unlike the overlying middle Cenomanian–lower Maastrichtian sequence of Western Interior ammonite/inoceramid zones, the late Albian–early Cenomanian interval beneath the Greenhorn Limestone and underlying Graneros Shale and equivalent strata are lithologically varied and discontinuous between different regions of the Western Interior Basin. These sedimentary rocks record the evolution of the Western Interior Seaway during ca. 10 Ma of the late Albian to early Cenomanian (Walaszczyk and Cobban, 2016; Fig. 1) but remain much less well known due to their limited biostratigraphy. The strata deposited during this interval are largely nearshore, shoreface sandstones or non-marine deposits and therefore lack the high-resolution biostratigraphy based upon marine ammonites and inoceramids. The paleontology and biostratigraphy of the marine tongues interlayered with the dominantly nonmarine sedimentary rocks have been recently reviewed by Walaszczyk and Cobban (2016). Some of these stratigraphic units are lithologically quite similar; thus, attempts to correlate them on the basis of lithology without independent evidence of age from fossils or geochronology may lead to highly uncertain correlations, as we document here based upon new radioisotopic ages.

Most of these lowest Western Interior Cretaceous rocks are stratigraphically associated with the Dakota Sandstone (Group) and the Skull Creek Shale, but the geochronologic data presented here include local units with different names in Colorado, Wyoming, Montana, and the Dakotas, USA, and in British Columbia. Although lithologically similar rocks occur in Utah, Kansas, Nebraska, and Iowa, USA, and in the Western Canada sedimentary basin (Alberta and British Columbia), we present no new geochronologic data from these states/provinces. Most of the new late Albian–early Cenomanian ages are from bentonite localities in Montana and Wyoming with a few correlated from Colorado (Fig. 2). In Wyoming, the succession of late Albian–early Cenomanian rocks includes the Thermopolis Shale, Muddy Sandstone, and Shell Creek Shale (Eicher,

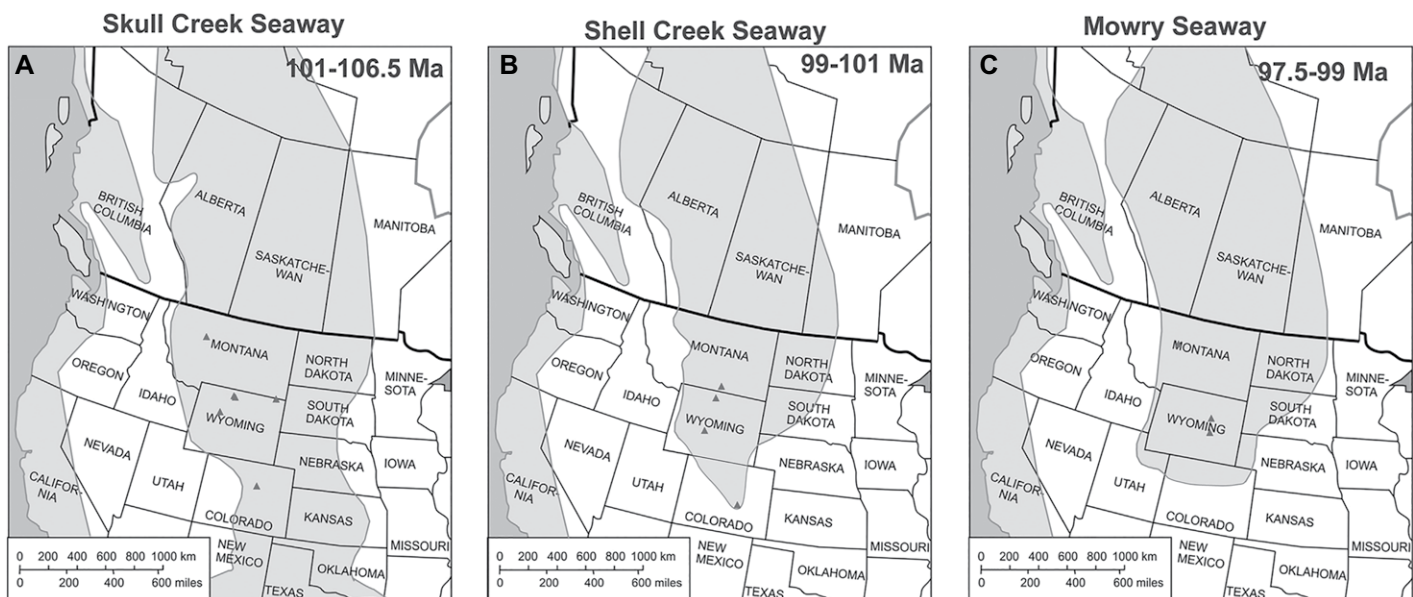


**Figure 1.** (A) Map shows the probable extent of the early late Albian Joli Fou/Skull Creek Seaway (*Gnesioceramus comancheanus* Zone) based on localities of *Gnesioceramus comancheanus* and *G. bellvuensis*. (B) Map shows the probable extent of the latest Albian earliest Cenomanian (Shell Creek time) Mowry Seaway (*Posidonioceramus nahwisi* Zone) and the ammonite zones of *Neogastropites haasi* and early *N. cornutus* based on localities of *Posidonioceramus nahwisi* (Walaszczyk and Cobban, 2016). (C) Map shows the probable extent of the early Cenomanian (Mowry Shale time) Mowry Seaway (*Gnesioceramus mowriensis* Zone; the ammonite zones of late *Neogastropites cornutus* through to *N. maclearni*) based on localities of *N. cornutus* and *N. maclearni*. See also Stott (1984) and Schroeder-Adams (2014). See alternate shoreline outlines in Oboh-Ikuenobe et al. (2008, their fig. 10) and Scott et al. (2009, their text and fig. 1).

1962) capped by the Mowry Shale (Reeside and Cobban, 1960). In the Sweetgrass Arch of northwestern Montana, Cobban et al. (1976) described the equivalent rocks as members of the Blackleaf Formation, specifically the Taft Hill, Vaughn, and Bootlegger Members (the last correlative with the Mowry Shale). Around the Black Hills and eastern Powder River Basin of Wyoming, South Dakota, and Montana, the succession is the Skull Creek Shale, Newcastle Sandstone, and Mowry Shale (Fig. 3). In the northern Colorado foothills, the stratigraphic succession of these late Albian and sparse early Cenomanian rocks are termed the Skull Creek Shale; the upper Dakota Sandstone is usually referred to as the Muddy or "J" Sandstone or as the South Platte Formation (Waagé, 1961; Higley et al., 2003). Older nonmarine clastic sedimentary rocks below the Skull Creek/Thermopolis Shale or their equivalents, and which lack biostratigraphic or isotopic geochronologic ages, include the Cloverly Formation; Lytle, Plainview, and Cheyenne Sandstones, the Inyan Kara Group, Lakota Formation, Burro Canyon, Buckhorn Formation, and Cedar Mountain Formations, lower Purgatoire Group, and Kootenai Group (Dolson and Muller, 1994, Fig. 3) and are not discussed further, as these sedimentary rocks are likely older than late Albian. Correlations to the Canadian strata equivalent to the

late Albian–early Cenomanian sequence in the U.S. Western Interior such as the Joli Fou Formation, Viking Sandstone, Bow Island Formation, and Fish Scales (Alberta Geological Society Western Canada Sedimentary Basin Atlas, Roca et al., 2008) will be discussed briefly but are not the principal focus of this paper (with one exception: redating the Peace River Ash in the Hulcross/Harmon Formation of British Columbia; Obradovich, 1993; Buckley and Plint, 2013). The major thrust of this paper is based on new  $^{40}\text{Ar}/^{39}\text{Ar}$  sanidine and  $^{206}\text{Pb}/^{238}\text{U}$  zircon ages for rocks in the northern Rocky Mountains and adjoining U.S. Great Plains. One European bentonite from the late Aptian (Gott claypit near Hannover, Germany, locality and sample from site 32 of Obradovich, 1993) has been redated and offers further constraints on the Aptian–Albian boundary interval in parallel with U-Pb zircon dates from the Vöhrum tuff, Germany (Selby et al., 2009).

There is abundant evidence for multiple unconformities and sequence boundaries throughout these non-marine and marginal marine sedimentary rocks that record the earliest transgression(s) of the Western Interior Seaway (Weimer, 1984). The clastic sandstone deposits of the Dakota Sandstone Group have been a principal target for petroleum exploration and have been developed as major oil and gas

reservoir rocks throughout the Rocky Mountains and adjoining Great Plains of New Mexico, Colorado, Wyoming, and Montana, USA, particularly during the second half of the 20th century (Weimer, 1996; Weimer et al., 1998; Dolson and Muller, 1994). The late Albian and Cenomanian sandstones in the western interior U.S. and Canada have produced over 3 billion barrels of oil and 11 trillion cubic feet of natural gas (Dolson and Muller, 1994; Fassett, 2014; Mossop and Shetsen, 1994). The intrinsic discontinuity of fluvial and near shore marine deposits has been detailed because of the abundant stratigraphic unconformity-bounded petroleum traps (Fig. 3). These have been mapped from outcrop and correlated into the subsurface where they are delineated in three dimensions by seismic stratigraphy and abundant exploration and production wells around many major and minor oil and gas fields (Higley et al., 2003). However, the scale and lateral extent of these unconformity-bound sequences is usually much smaller than the distance between outcrop exposures and petroleum-producing zones, so that the seismically defined sequence boundaries, locally captured in cores drilled for exploration or reservoir characterization, have substantial uncertainty in the correlation to the surface or between basins. Nevertheless, the outcrop lithologies and contact relations with unconformities provide important analogs

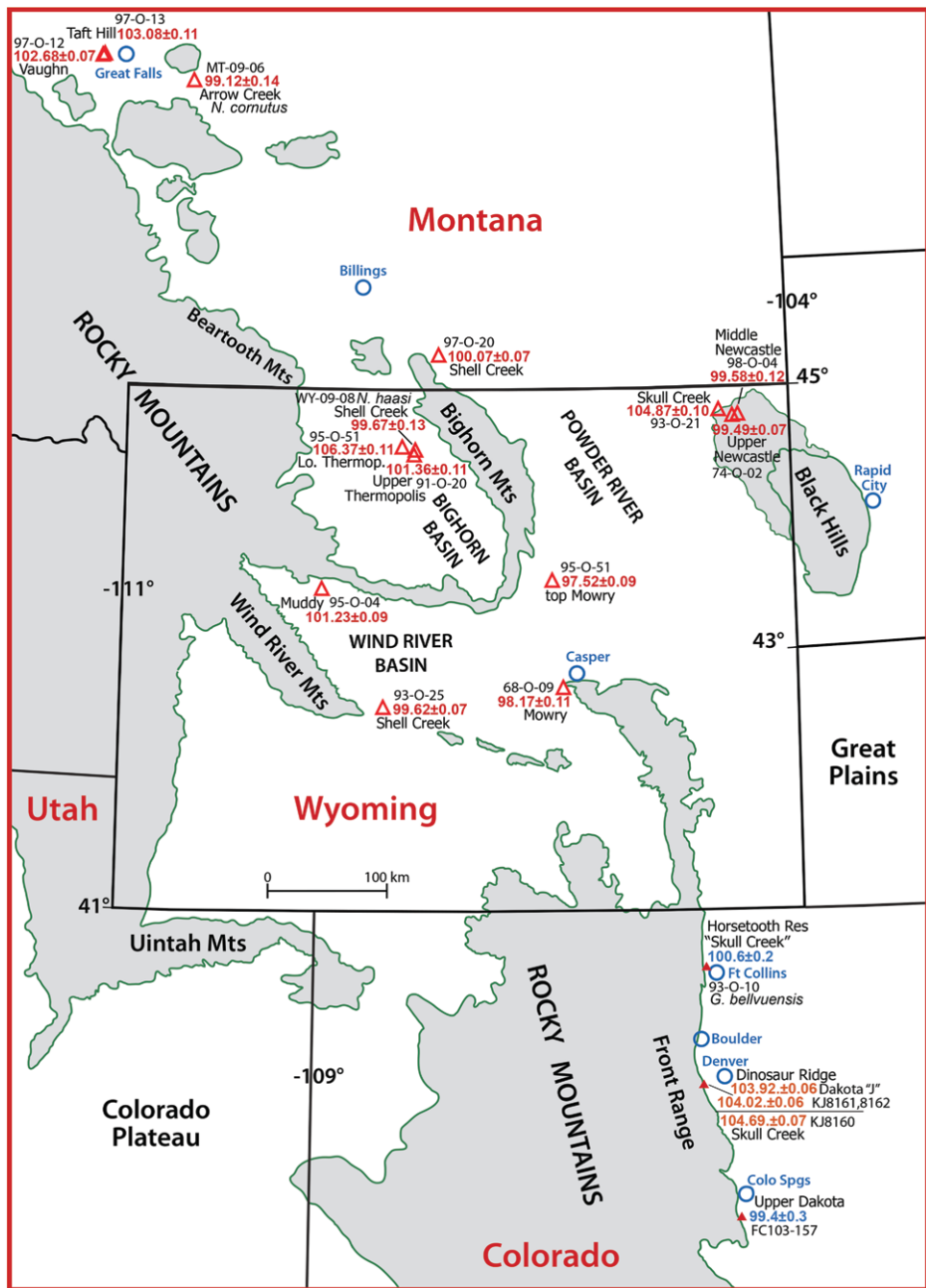


**Figure 2.** Location map shows new ages of rocks of the late Albian–early Cenomanian interval in Montana, Wyoming, and Colorado, USA. Bentonite ages are represented by red open triangles for new high-resolution, multi-collector mass spectrometer ages, and solid red triangles in Colorado show where there are new U-Pb ages of zircon and older  $^{40}\text{Ar}/^{39}\text{Ar}$  ages of sanidine, recalculated to contemporary Fish Canyon sanidine monitor ages of 28.201 Ma. Cities of the central and northern Rockies are indicated, as are the locations of the major basins in north central Wyoming: Bighorn, Wind River, and Powder River Basins. Sample # and stratigraphic unit are listed for each sample (Table 1).

for understanding facies relationships and geometries in the oil- and gas-producing basins.

While the stratigraphy, sedimentology, and petrophysical properties of late Albian–Cenomanian sedimentary sequences are often well-characterized within and adjoining the petro-

leum reservoir systems, the lateral extent and amount of time missing between sequences is fundamentally unknown. The amount of time missing between these sequences has not been constrained in detail anywhere by radioisotopic geochronology or even high-resolution biostra-

tigraphy. To constrain the amount of time represented by unconformities, it would be necessary to determine ages in the top and bottom of lower-order parasequences bounding the unconformities. While this paper provides the most detailed radioisotopic dating attempted for these late Albian–Cenomanian sedimentary rocks in the Western Interior Basin, it also demonstrates that many correlations based on lithology are not temporally coeval and thus not sedimentologically equivalent sequence stratigraphic units.

#### Age of the Albian–Cenomanian Boundary

The Global Boundary Stratotype Section and Point (GSSP) for the base of the Cenomanian was ratified by the International Commission on Stratigraphy in 2004 (Kennedy et al., 2004) at Mont Risou near Rosans, Haute-Alpes, in southern France in the top of the Marnes Bleus Formation. It is defined with the first occurrence (FO) of the planktonic foraminifera *Thalmanninella globotruncanoides* (formerly *Rotalipora globotruncanoides*; see, e.g., Petrizzo et al., 2015). Other, secondary markers of the boundary include the last occurrence (LO) of the upper Albian planktonic foraminifera *Pseudothalmanninella tictinensis* (formerly *Rotalipora tictinensis*) and the FOs of *Thalmanninella gandolfii* (formerly *Rotalipora gandolfii*), *Thalmanninella brotzeni* (formerly *Rotalipora brotzeni*), and *Pseudothalmanninella tehamaensis* (formerly *Rotalipora tehamaensis*) (Petrizzo et al., 2015). The FO of the characteristic lower Cenomanian ammonite *Mantliceras mantelli* post-dates the FO of *T. globotruncanoides* by 6 m. Also of potential correlation significance are a high-resolution, carbon-isotope curve across the boundary with four characteristic Albian–Cenomanian boundary peaks (Gale et al., 1996; Kennedy et al., 2004; Kennedy and Gale, 2006; Gale et al., 2011) and astronomical calibration of the duration of European ammonite zones.

Unfortunately, the GSSP for the Albian–Cenomanian boundary at Mont Risou is completely lacking in bentonites and thus unsuitable for direct calibration by radioisotopic dating. In the North American Western Interior, the boundary diagnostic planktonic foraminifera, calcareous nannofossils, ammonites, and inoceramids are not present, and an uncertain amount of time is missing across multiple upper Albian and lower Cenomanian unconformities. The sections in the western Canada sedimentary basin and in the transitional U.S. Western Interior Basin have only limited biostratigraphic control of the ammonite genus *Neogastropolites* (Reeside and Cobban, 1960) and of endemic lineages of inoceramid bivalves (Walaszczuk and Cobban, 2016). The Tethyan, circum-Caribbean, and

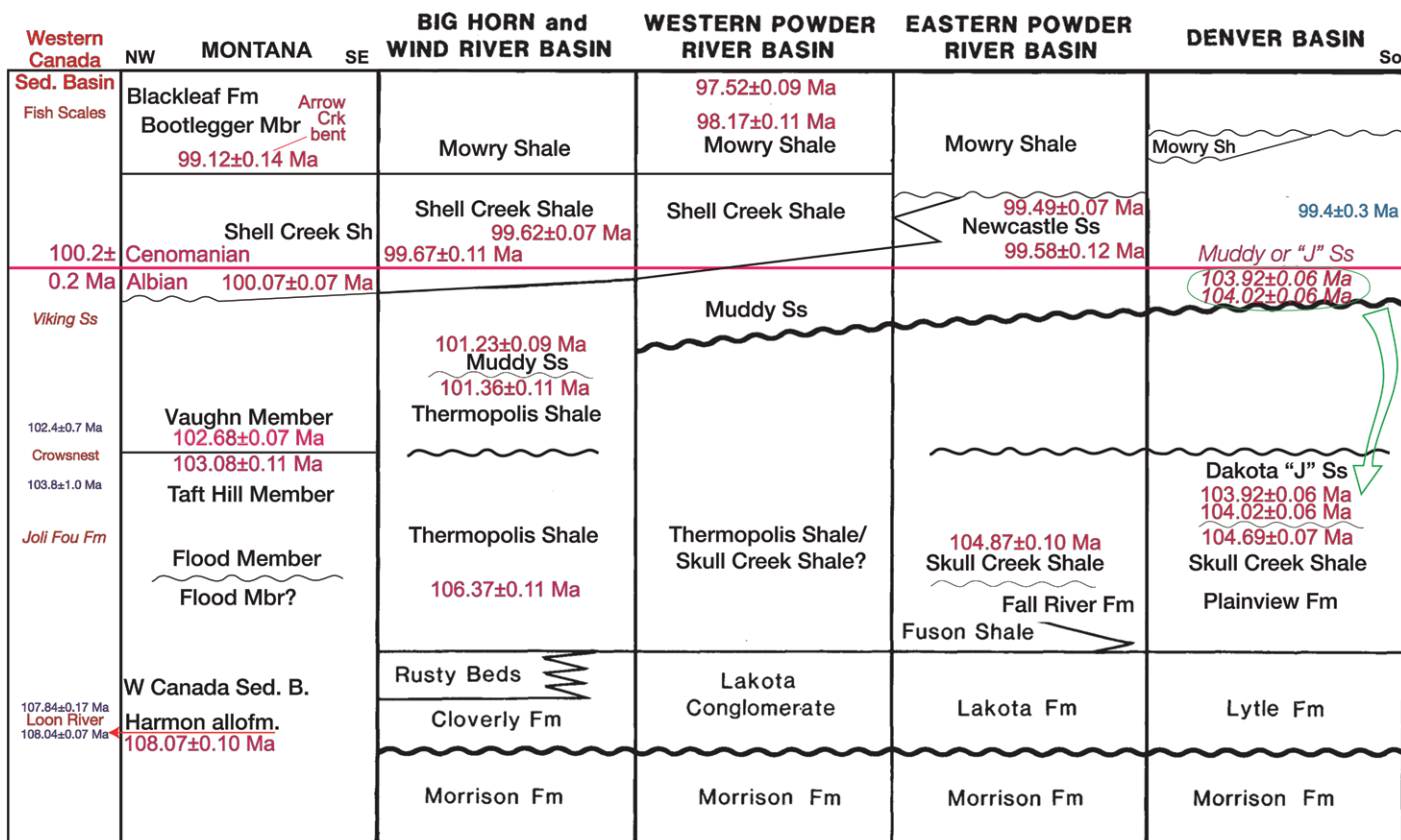


Figure 3. Albian–lower Cenomanian stratigraphic chart after Gustason (1988) of the Cretaceous Western Interior in Colorado, Wyoming, and Montana, USA, with correlation to the Western Canada Sedimentary Basin (Walaszczyk and Cobban, 2016) shows new age determinations. The most significant change is the shift in the age of the Dakota “J” Sandstone at Dinosaur Ridge such that it cannot be correlative with the Newcastle Sandstone of the Powder River Basin or the Muddy Sandstone of the north central Wyoming Wind River and Bighorn Basins. The Dakota “J” Sandstone may, however, be closer in age to the subjacent Skull Creek Shale in the northwest Black Hills of Wyoming and the Denver Basin Dinosaur Ridge section. The Skull Creek Shale, Kassler Member of the Dakota “J” Sandstone, Taft Hill and Vaughn Members of the Blackleaf Formation, as well as the Uppermost Thermopolis Shale in the Bighorn Basin and Muddy Sandstone at Maverick Springs Dome in the Wind River Basin are each late Albian in age. The Lower Thermopolis Shale in the Bighorn Basin and the Peace River Ash (Harmon alloformation) straddle the boundary between the lowest late Albian and the middle Albian. Earliest Cenomanian rocks include the Shell Creek Shale and the Newcastle Sandstone and younger lower Cenomanian rocks associated with the Mowry Shale. The Albian–Cenomanian boundary likely occurs in rocks described as the Shell Creek Shale (Eicher, 1960, 1962); the four ages we report from the Shell Creek extend from 100.07 Ma through 99.12 Ma. The oldest age for the Mowry Shale is based upon the Arrow Creek Bentonite, which is immediately beneath the Bootlegger Member of the Blackleaf Formation in north central Montana and is 99.14 Ma. It is not certain that this is correlative with the base of the Mowry Shale in north central Wyoming or in the Powder River Basin. Ages in the middle to upper Mowry in Wyoming range from 98.17 Ma to 97.52 Ma and do not support a correlation of the uppermost Mowry Bentonite as a precise time marker locally or regionally. Ss—sandstone; Fm—formation; Mbr—member; Sed. B.—Sedimentary Basin; Sh—shale; allof.—alloformation.

Ocean Drilling Program marine planktonic foraminifera and calcareous nannofossil biostratigraphic framework (Ogg and Hinnov, 2012) does not range far enough north to be correlated with the European type sections or the Western Interior Cretaceous Basin. Consequently, the age of the base of the Cenomanian stage has been difficult to accurately establish. Obradovich (1993) demonstrated that there are datable bentonites present in the upper Albian–lower Cenomanian associated with the *Neogastropolites* ammonite fauna and associated with the bentonite-rich Mowry Shale. More recently, Walaszczyk and

Cobban (2016) published an inoceramid biostratigraphy of the upper Albian–Cenomanian, and it is within their framework that we present new  $^{40}\text{Ar}/^{39}\text{Ar}$  dates.

Critical biostratigraphic evidence from Japan on the age of the Albian–Cenomanian boundary was provided by Tatsuro Matsumoto (1913–2009) and calibrated by  $^{40}\text{Ar}/^{39}\text{Ar}$  dating in Obradovich et al. (2002). Biostratigraphically constrained bentonites were obtained from the Cretaceous Yezo Group of Hokkaido, Japan. The lowest occurrence of *T. globotruncanoides* was directly dated by a  $^{40}\text{Ar}/^{39}\text{Ar}$  bentonite

age of  $99.99 \pm 0.37$  Ma (recalculated relative to 28.201 Ma FCs from the date in Cobban et al., 2006). The key GSSP correlation of the first occurrence of the index planktonic foraminifera was succeeded in the Japanese section by the FO of the ammonite *Graysonites wooldridgei* (= *Graysonites wacoense*; see Kennedy et al., 2004), which is broadly correlative with the base of the European *Mantelliceras mantelli* ammonite zone. Higher in the section, a second bentonite age of  $99.66 \pm 0.40$  Ma recalculated from the ammonite zone of *Mantelliceras saxbii* is found directly overlying the *Mantelliceras*

*mantelli* zone in the European succession. On the strength of these bentonite dates calibrating the planktonic foraminifera age for the base of the Cenomanian, Ogg and Hinnov (2012) placed the Albian–Cenomanian boundary at  $100.5 \pm 0.5$  Ma in GTS2012.

This older ca. 100 Ma age for the Albian–Cenomanian boundary conflicted with the historic usage of the bentonite atop the Mowry Shale (Clay Spur Bentonite in the Western Interior U.S.; Fish Scales Formation in Canada) as demarcating the Albian–Cenomanian boundary. Obradovich (1993) had determined the age of the Clay Spur Bentonite outside of Casper, Natrona County, Wyoming, to be 97.73 Ma (relative to 28.201 Ma FCs). This much younger top of the Albian stage persisted in the literature, despite Obradovich (1993) arguing that ammonite biostratigraphy indicates a minimum age for the Albian–Cenomanian boundary in the range of ca. 98.5–99 Ma (not recalibrated). The Geologic Time Scale 2004 (GTS04, Gradstein et al., 2004) also moved the probable age of the Albian–Cenomanian boundary older to  $99.6 \pm 0.9$  Ma (not recalibrated). Only recently (Scott et al., 2018; Plint et al., 2018) has the placement of the Albian–Cenomanian boundary below the Mowry Shale/Fish Scales Formation been widely accepted, and it is now as much as 2–3 Ma older than originally inferred from the Obradovich (1993) Clay Spur Bentonite date close to 97 Ma. The new ages presented here better define the exact correlation of the Albian–Cenomanian boundary within the stratigraphic framework of the Western Interior Seaway, as discussed below.

## Previous Geochronology

In the U.S. Western Interior, the lowest dated bentonite that can be reliably tied to the continuous Upper Cretaceous ammonite-inoceramid biostratigraphy (Cobban et al., 2006) is the *Conlinoceras tarrantense* (previously *Conlinoceras gilberti*) Bentonite, immediately below the Thatcher limestone bed in the Granos Shale of the Pueblo Upper Cretaceous reference section (Cobban et al., 2006; Obradovich 1993). It is dated at  $96.21 \pm 0.16$  Ma (Batenburg et al., 2016), with the overlying *Acanthoceras amphibolum* Zone X Bentonite dated at  $95.53 \pm 0.09$  Ma (Ogg and Hinnov, 2012) and the lowest Upper Cenomanian *Dunveganoceras pondi* Zone Bentonite dated at  $95.39 \pm 0.18$  Ma (Ma et al., 2014). These ages were each determined using a single collector mass spectrometer at the WiscAr Laboratory prior to 2014.

Other bentonite ages relevant to the lower Cenomanian and late Albian of the Western Interior Basin were reported in Obradovich (1993) without supporting metadata. These include

recalibrated ages of  $96.5 \pm 0.5$  Ma (originally reported as 95.86 Ma) from a bentonite 27 m (88 ft) below the lowest *Conlinoceras tarrantense* (*C. gilberti*) occurrence in the Bailey Flats core drilled in Frontier Formation of the Powder River Basin, Johnson County, Wyoming. An age from near the local top of the Mowry Shale in Natrona County, Wyoming sample, reputedly the “Clayspur” Bentonite bed, yields a recalibrated age of  $97.8 \pm 0.7$  Ma (originally 97.17 Ma). Ages were reported from two samples of bentonite associated with the *Neogastropolites* ammonite lineage, and one additional age more questionably correlated to the Neogastropolites. Two bentonites of earlier Albian and late Aptian age were reported from outside the U.S. Western Interior in Canada and Germany; these samples all have new ages reported below and will be discussed after presentation of the new  $^{40}\text{Ar}/^{39}\text{Ar}$  and  $^{206}\text{Pb}/^{238}\text{U}$  results.

## GEOCHRONOLOGY

### Samples

We report new  $^{40}\text{Ar}/^{39}\text{Ar}$  dates from single crystals of sanidine in 16 bentonitic volcanic ash beds and new  $^{206}\text{Pb}/^{238}\text{U}$  dates from single zircon crystals in three other horizons. Thirteen of the samples were collected from late Albian and early Cenomanian strata of the Western Interior Basin in Wyoming, Montana, and Alberta by Bill Cobban and John Obradovich. Two were collected by Brad Singer, Brian Jicha, and Sarah Siewert from localities 28 and 29 of Obradovich (1993). One sample from Gott, Germany, within late Aptian strata was provided to Obradovich (Obradovich, 1993). The samples from the Dakota Sandstone at Dinosaur Ridge, Colorado, were collected for U-Pb dating by Sam Bowring and Kirk Johnson. We subsequently collected these tuffs at Dinosaur Ridge but could not separate sanidine from them likely due to low-temperature, silica-clay acid alteration of the feldspars in a nonmarine deposit. For comparison, we also note the  $^{40}\text{Ar}/^{39}\text{Ar}$  date from a bentonite in the Dakota Sandstone at Deadman Canyon, Colorado, that was collected by Robert W. Scott and John M. Holbrook, dated by Obradovich, and published in Oboh-Ikuenobe et al. (2008). The location and stratigraphic context of each ash bed are summarized in Figure 2 and Table 1, and more detailed description of the local stratigraphy is provided in the Supplementary Materials<sup>1</sup>.

<sup>1</sup>Supplemental Material. Figures S1–S15 and Tables S1–S2. Please visit <https://doi.org/10.1130/GSAB.S.13063922> to access the supplemental material, and contact [editing@geosociety.org](mailto:editing@geosociety.org) with any questions.

### $^{40}\text{Ar}/^{39}\text{Ar}$ Methods

Sanidine separates, obtained using the methods of Sageman et al. (2014), were wrapped in aluminum foil, placed in one of 17 wells each 4 mm in diameter and cut into a 4-mm-thick aluminum disk that is 2.5 cm in diameter. In each well several crystals of the  $28.201 \pm 0.046$  Ma FCs sanidine standard (Kuiper et al., 2008) were placed with the samples. Irradiations occurred over a period of several years at the Oregon State University TRIGA reactor in the Cadmium-Lined In-Core Irradiation Tube (CLICIT). Single crystal fusion experiments in the WiscAr Laboratory at the University of Wisconsin–Madison were undertaken with a 50 W  $\text{CO}_2$  laser followed by gas analysis in a Noblesse multi-collector mass spectrometer via procedures in Jicha et al. (2016). For two samples, MT-09-06 from the Arrow Creek Bentonite in Montana, and WY-09-08 from a bentonite in the Shell Creek Shale in Wyoming, single-collector mass spectrometry methods as in Sageman et al. (2014) were used. *J* values were determined for each sample based on single crystal analyses of 4–8 FCs monitors in each well of the irradiation disk. No interpolation or modeling of *J* values was attempted because the samples and monitor were co-located in the same well. Procedural blanks were typically 3000 cps (0.5 fA) for  $^{40}\text{Ar}$  and 12 cps (0.002 fA) for  $^{36}\text{Ar}$  and were measured before and after each single crystal fusion. The average of the two bracketing blanks was subtracted from the sample and monitor measurements.

The isotopic composition of atmospheric argon used to calculate radiogenic argon percentages is from Lee et al. (2006). Ages are calculated using the decay constants of Min et al. (2000) and are reported as  $\pm X/Y/Z$ , where *X* is the internal analytical uncertainty at the 95% confidence level, *Y* is this internal uncertainty plus that contributed by the measurement of the *J* value, and *Z* is the total uncertainty, which includes the internal and *J* value uncertainties plus systematic contributions from uncertainty in the  $^{40}\text{K}$  decay constant and age of the FCs standard. The total uncertainties are calculated using the ArAR software program (Mercer and Hodges, 2016).

### U-Pb Methods

Zircon grains were separated from bulk rock samples by standard crushing, heavy liquid, and magnetic separation techniques and subsequently handpicked under the binocular microscope based on clarity and crystal morphology. To minimize the effects of Pb loss, the grains were subjected to a version of the thermal

TABLE 1. SAMPLE DESCRIPTION AND SUMMARY OF SINGLE SANIDINE  $^{40}\text{Ar}/^{39}\text{Ar}$  AND SINGLE ZIRCON U-Pb EXPERIMENTS

Sample	Ob93	Sample/Stratigraphic description/Ammomite zone	Location	Latitude (°N)	Longitude (°W)	Elevation (m)	N	MSWD	Age (Ma)	$\pm 2\sigma_{\text{int}}$	$\pm 2\sigma_{\text{int+J}}$	$\pm 2\sigma_{\text{tot}}$
$^{40}\text{Ar}/^{39}\text{Ar}$ results*												
90-O-51		Topmost bentonite, Mowry Shale, near Kaycee "Clay Spur" Bentonite, local top of Mowry Shale	Johnson County, Wyoming, USA	43.57196	-106.580043	1492	9 of 18	0.90	97.52	$\pm 0.04$	$\pm 0.09$	$\pm 0.17$
68-O-09	27	"Clay Spur" Bentonite, local top of Mowry Shale	Natrona County, Wyoming	42.76562	-106.47278	1684	8 of 8	0.83	98.17	$\pm 0.07$	$\pm 0.11$	$\pm 0.19$
MT-09-06	~28	Arrow Creek Bentonite, Colorado Shale, <i>Neogastropilites cornutus</i> Member, lower upper Dakota Sandstone	Judith Basin County, Montana, USA	47.31464	-110.485666	1233	11 of 11	0.18	99.12	$\pm 0.10$	$\pm 0.14$	$\pm 0.21$
7JDO35†		Dry Creek Canyon Member, lower upper Dakota Sandstone	Deadman Cany., El Paso Cnty., Colo., USA	38.67285	-104.854969	1917	6 of 8		99.37		$\pm 0.31$	$\pm 0.35$
74-O-02		Newcastle Sandstone—upper bentonite	Crook County, Wyoming	44.79557	-104.65863	1327	15 of 22	1.11	99.49	$\pm 0.03$	$\pm 0.07$	$\pm 0.17$
98-O-04		Newcastle Sandstone—middle bentonite	Crook County, Wyoming	44.79157	-104.66985	1352	11 of 24	0.70	99.58	$\pm 0.03$	$\pm 0.12$	$\pm 0.19$
93-O-25		Shell Creek Shale, Southeast of Lander, US 287, above Muddy Ss	Fremont County, Wyoming	42.61224	-108.322463	1855	11 of 16	0.80	99.62	$\pm 0.03$	$\pm 0.07$	$\pm 0.17$
WY-09-08	~29	Upper Shell Creek Shale, NE of Greybull, <i>Neogastropilites haasi</i>	Big Horn County, Wyoming	44.55326	-107.99181	1290	20 of 21	0.74	99.67	$\pm 0.11$	$\pm 0.13$	$\pm 0.20$
97-O-20		Shell Creek Shale, basal bentonite, Soap Creek Dome, Crow I.R.	Big Horn County, Montana	45.26738	-107.758751	1116	14 of 15	1.70	100.07	$\pm 0.03$	$\pm 0.07$	$\pm 0.17$
95-O-04		Muddy Sandstone, upper of 2 upper bentonites, Maverick Springs	Dome, Fremont County, Wyoming	43.51363	-108.961752	2022	4 of 24	0.78	101.23	$\pm 0.05$	$\pm 0.09$	$\pm 0.18$
97-O-01		Uppermost Thermopolis Shale just below Muddy Sandstone	Greybull, Big Horn County, Wyoming	44.52660	-108.00360	1200	5 of 19	0.74	101.36	$\pm 0.05$	$\pm 0.11$	$\pm 0.19$
97-O-12		2.2–1.5-ft-thick, water-lain tuff in Mid-Vaughn Memb., Blackleaf Fm.	So. of Vaughn, Cascade Cnty., Montana	47.49533	-111.53023	1124	17 of 43	0.26	102.68	$\pm 0.03$	$\pm 0.07$	$\pm 0.18$
97-O-13		Taft Hill Member bed 27, 48 ft below top of Taft Hill, Blackleaf Fm.	So. of Vaughn, Cascade Cnty., Montana	47.50114	-111.530316	1099	11 of 21	0.50	103.08	$\pm 0.03$	$\pm 0.11$	$\pm 0.20$
93-O-21		~4" bentonite, 7 ft above base of Skull Creek Shale	Devils Tower, Crook County, Wyoming	44.81882	-104.741437	1169	12 of 18	0.87	104.87	$\pm 0.04$	$\pm 0.10$	$\pm 0.19$
98-O-08		Green marker bentonite, Lower Thermopolis Shale, NW of Greybull	Big Horn County, Wyoming	44.57564	-108.135273	1186	15 of 20	1.50	106.37	$\pm 0.04$	$\pm 0.11$	$\pm 0.20$
75-O-06	31	50 m below top Hulcross Fm., <i>Pseudopulchellia pattoni</i>	Hudson's Hope, BC, Canada	56.10752	-121.817888	607	7 of 24	0.59	108.07	$\pm 0.05$	$\pm 0.10$	$\pm 0.20$
Gott	32	Thin bentonite Otto Gott clay pit, <i>Parahoplitops nutfieldensis</i>	21 km SE of Hannover, Germany	52.24838	9.88267°E	97	24 of 44	1.12	114.77	$\pm 0.15$	$\pm 0.17$	$\pm 0.26$
$^{206}\text{Pb}/^{238}\text{U}$ results												
KJ08162		Kassler Member, Dakota "J" Sandstone, No. side Alameda roadcut	Dinosaur Ridge, Jefferson Cnty., Colo.	39.67582	-105.192518	1883	5 of 5	0.06	103.92	$\pm 0.04$	$\pm 0.06$	$\pm 0.13$
KJ08161		Kassler Member, Dakota "J" Sandstone, So. side Alameda roadcut	Dinosaur Ridge, Jefferson Cnty., Colo.	39.67563	-105.192582	1884	11 of 11	0.72	104.02	$\pm 0.04$	$\pm 0.06$	$\pm 0.13$
KJ08160		Skull Creek Member, Dakota Sandstone, South side roadcut	Dinosaur Ridge, Jefferson Cnty., Colo.	39.67578	-105.193111	1882	6 of 6	0.03	104.69	$\pm 0.05$	$\pm 0.07$	$\pm 0.13$

Notes: N—number of single crystal fusion dates used for age calculation relative to the total number of dates. Ob93—Location from table II of Obradovich (1993).  $\pm 2\sigma_{\text{int}}$ —analytical uncertainty only at the 95% confidence interval.  $\pm 2\sigma_{\text{int+J}}$ —analytical uncertainty at the 95% confidence interval including J uncertainty.  $\pm 2\sigma_{\text{tr}}$ —analytical plus tracer uncertainty.  $\pm 2\sigma_{\text{tot}}$ —fully propagated uncertainty at the 95% confidence interval including analytical, tracer/standard age, and decay constant uncertainties. MSWD—mean square of weighted deviations; Cany.—canyon; Cnty.—county; Memb.—member; Fm.—formation; Ss—sandstone; Colo.—Colorado.

\*Ages calculated relative to 28.201 Ma Fish Canyon sanidine standard (Kuiper et al., 2008) using Min et al. (2000) decay constants.

†Data from Oboh-Ikuenobe et al. (2008).

annealing and acid leaching (also known as chemical abrasion-thermal ionization mass spectrometry or CA-TIMS) technique of Mattinson (2005) prior to isotope dilution-thermal ionization mass spectrometry (ID-TIMS) analyses using a mixed  $^{205}\text{Pb}$ - $^{233}\text{U}$ - $^{235}\text{U}$  tracer solution (spike). Details of zircon pre-treatment, dissolution, and U and Pb chemical extraction procedures are described in Ramezani et al. (2007). U and Pb isotopic measurements were

performed on a VG Sector-54 multi-collector-thermal ionization mass spectrometer at MIT. Pb and U were loaded together on a single Re filament in a silica-gel/phosphoric acid mixture (Gerstenberger and Haase, 1997). Pb isotopes were measured by peak-hopping using a single Daly photomultiplier detector, and U isotopic measurements were made in static mode using multiple Faraday collectors. Details of fractionation and blank corrections are given in Table S2

(see footnote 12). Data reduction, age calculation, and the generation of concordia plots were carried out using the method of McLean et al. (2011) and the statistical reduction and plotting program REDUX (Bowring et al., 2011). Unless otherwise noted, U-Pb errors on analyses from this study are reported as  $\pm X/Y/Z$ , where X is the internal uncertainty in the absence of all systematic uncertainty, Y includes the tracer calibration uncertainty, and Z includes both the tracer

calibration and decay constant uncertainties of Jaffey et al. (1971).

## RESULTS

The  $^{40}\text{Ar}/^{39}\text{Ar}$  and  $^{206}\text{Pb}/^{238}\text{U}$  results are summarized in Table 1 with complete data in Tables S1 and S2 (see footnote 1). Between eight and 44 individual sanidine crystals were measured from each sample using the Noblesse mass spectrometer. With the exception of the  $98.17 \pm 0.07/0.11/0.19$  Ma Mowry Bentonite 68-O-09 (Table 1, Fig. 4), the  $^{40}\text{Ar}/^{39}\text{Ar}$  dates for the other samples show dispersion, most prominently with “tails” toward dates significantly older than the youngest crystals, and in these samples the youngest group of dates that yield a statistically reasonable mean square weighted deviation (MSWD) are used to calculate an inverse variance weighted mean date that we interpret to be the time elapsed since eruption and deposition of the ash (Fig. 4). We interpret the crystals that give dates younger than the larger group of relatively young dates as reflecting argon loss due to weathering or low temperature alteration. We interpret the crystals older than those yielding statistically identical dates as either detrital grains or inherited crystals incorporated into the eruption column or during reworking of the deposit at the surface (e.g., Schaen et al., 2020; Fig. 4). The two samples measured by single-collector mass spectrometry yield fairly homogeneous sets of dates. New ages include:  $97.52 \pm 0.04/0.09/0.17$  Ma for the Clayspur Bentonite (sample 90-O-51),  $99.49 \pm 0.03/0.07/0.17$  Ma for an upper Newcastle Sandstone Bentonite (74-O-02), and  $99.58 \pm 0.03/0.12/0.19$  Ma for a middle Newcastle Sandstone Bentonite (98-O-04). There are three bentonites in the Shell Creek Shale that provide ages of  $99.62 \pm 0.03/0.07/0.17$  Ma (90-O-25),  $99.67 \pm 0.11/0.13/0.20$  Ma (WY-09-08), and  $100.07 \pm 0.03/0.07/0.17$  Ma (97-O-20). The upper bentonite in the Muddy in the Wind River Basin gives an age of  $101.23 \pm 0.05/0.09/0.18$  Ma. A bentonite in the uppermost Thermopolis Shale (97-O-01), immediately beneath the Muddy Sandstone at Greybull, Wyoming, has an age of  $101.36 \pm 0.05/0.09/0.19$  Ma. A bentonite in the middle of the Vaughn member (97-O-12) yields an age of  $102.68 \pm 0.03/0.07/0.18$  Ma. We note that the latter is based on 12 dates that are older than the youngest four dates, which yield an age of  $102.12 \pm 0.05/0.12/0.20$  Ma. Our preferred age for the Vaughn member is based on the larger number of crystals (Table 1; Fig. 4). The Taft Hill Member bed 27 (93-O-25) is dated at  $103.08 \pm 0.03/0.11/0.20$  Ma, whereas a bentonite in the basal Skull Creek Shale in

the northwest Black Hills (93-O-21) yields an age of  $104.87 \pm 0.04/0.10/0.19$  Ma. A bentonite in the Lower Thermopolis Shale yields an age of (98-O-08)  $106.37 \pm 0.04/0.11/0.20$  Ma and one in the Hulcross Formation (Harmon alloformation), British Columbia (75-O-06), is  $108.07 \pm 0.05/0.11/0.20$  Ma. The result from a Gott quarry sample in upper Aptian strata, Germany, is  $114.81 \pm 0.15/0.17/0.26$  Ma (Table 1, Fig. 4).

Between five and 11 zircon crystals in each of the three tuffs at Dinosaur Ridge, Colorado, were measured with  $^{206}\text{Pb}/^{238}\text{U}$  dates in each sample yielding statistically indistinguishable results and inverse-variance weighted mean dates of  $103.92 \pm 0.04/0.063/0.130$  Ma,  $104.02 \pm 0.04/0.059/0.130$  Ma, and  $104.69 \pm 0.05/0.072/0.130$  Ma (Table 1; complete U-Pb isotopic data and concordia plots are in Table S2 (see footnote 1). Given the total uncertainties of the  $^{40}\text{Ar}/^{39}\text{Ar}$  ages, the  $^{206}\text{Pb}/^{238}\text{U}$  age of the Skull Creek member sample KJ08160 from Colorado of  $104.69 \pm 0.05/0.072/0.130$  Ma is indistinguishable from the  $^{40}\text{Ar}/^{39}\text{Ar}$  age of  $104.87 \pm 0.05/0.18$  Ma for sample 93-O-21 in the Skull Creek Shale in Wyoming (Fig. 4). Notably, sample 7JDO35 from the Dakota Sandstone equivalent to the Muddy J in Colorado, measured by Obradovich (Oboh-Ikuenobe et al., 2008), yields an  $^{40}\text{Ar}/^{39}\text{Ar}$  date of  $99.4 \pm 0.4$  Ma (total uncertainty). This age is ca. 4 Ma younger than either of the two ash beds within Muddy J Dakota Sandstone at Dinosaur Ridge, Colorado, whose  $^{206}\text{Pb}/^{238}\text{U}$  dates are  $103.92 \pm 0.13$  Ma and  $104.02 \pm 0.13$  Ma (total uncertainty).

## DISCUSSION

The radioisotopic ages in Table 1 comprise the largest set determined from Cretaceous rocks spanning the upper Albian and Cenomanian substages (Figs. 2 and 4). Here we discuss the implications of our results from the youngest to oldest of the dated bentonites. The youngest are from the Mowry Shale of central Wyoming. The highest thick bentonite in the Mowry Shale is commonly called the “Clay Spur” Bentonite and is described as “the topmost bed of the Mowry Shale at most places on the northern and western flanks of the Black Hills, Wyoming, Montana, and South Dakota” (Robinson et al., 1964), where it is mined as the principal source of commercial and industrial bentonite. Knechtel and Patterson (1955) called the bentonite mined in this area “the world’s best-known and most productive bentonite district” and “the greater part of this country’s known minable reserve.” Regionally, the “Clay Spur” Bentonite ranges from 0.7 m to 1.3 m in thickness but varies locally between 3 cm to 2.3 m thick. It grades

upward into as much as 2 m of the siliceous sediment characteristic of the Mowry Shale beneath the overlying dark, non-siliceous sediment of the Belle Fourche Shale Member of the Frontier Formation. As expanded upon below, numerous later studies have, perhaps incorrectly, correlated the reported “top bentonite bed” of the Mowry Shale to the Clay Spur Bentonite throughout Wyoming and into Utah, North Dakota, and Colorado. Subsequently, it was also correlated into the Western Canada Sedimentary Basin as the equivalent of the “Fish Scales.”

The name “Mowry” was used first by Darton (1904) as a member of the Benton Group northwest of Buffalo, Wyoming, on the west side of the Powder River Basin; no type section was or ever has been designated. As with many Cretaceous stratigraphic units for which no type section has been designated, the stratigraphic name Mowry has been used in a wide variety of stratigraphic ranks and contexts (as is the case for the stratigraphic units Mancos and Mesaverde, or arguably even Dakota, Niobrara, and Pierre). The two ages we have determined on bentonites near the top of the Mowry Shale in central Wyoming are examples of the consequences of the colloquial use of stratigraphic names. The first example is a re-dating of the bentonite (sample 68-O-09) collected by John Obradovich in 1968 from an outcrop on Wyoming Highway 220, 12.9 km southwest of Casper, Natrona County, Wyoming, which was most recently dated by Obradovich (1993) at  $97.17 \pm 0.69$  Ma (recalibrated to 97.80). The outcrop from which Obradovich collected the sample was destroyed when the highway was widened from two lanes to four lanes. Redating his original sanidine yields an age of  $98.17 \pm 0.07/0.11/0.19$  Ma (Table 1). We also dated another sample, (90-O-51), collected by W.A. Cobban and E.A. Merewether at the top of the Mowry Shale near Kaycee, Wyoming, (Thorson, 1976) that yields an age of  $97.52 \pm 0.04/0.09/0.17$  Ma (Fig. S2; see footnote 1). These two bentonites are thus distinct from one another by  $650 \pm 20$  ka. They are both from the Casper Arch region, less than 100 km apart, and from the topmost thick bentonite of the Mowry Shale. Yet, based upon the new age determinations, they are neither temporally nor stratigraphically equivalent. We suggest that the so-called “Clay Spur” Bentonite not be correlated out of the northwest Black Hills region of Wyoming, South Dakota, and Montana (Allison, 1988). To be certain of correlation of bentonite beds in the Mowry Shale, one must use tephrochronology methods to test whether two bentonites are actually stratigraphically equivalent, including mineral chemistry and radioisotopic ages from minerals, because no primary volcanic glass has survived. The topmost bentonite in the

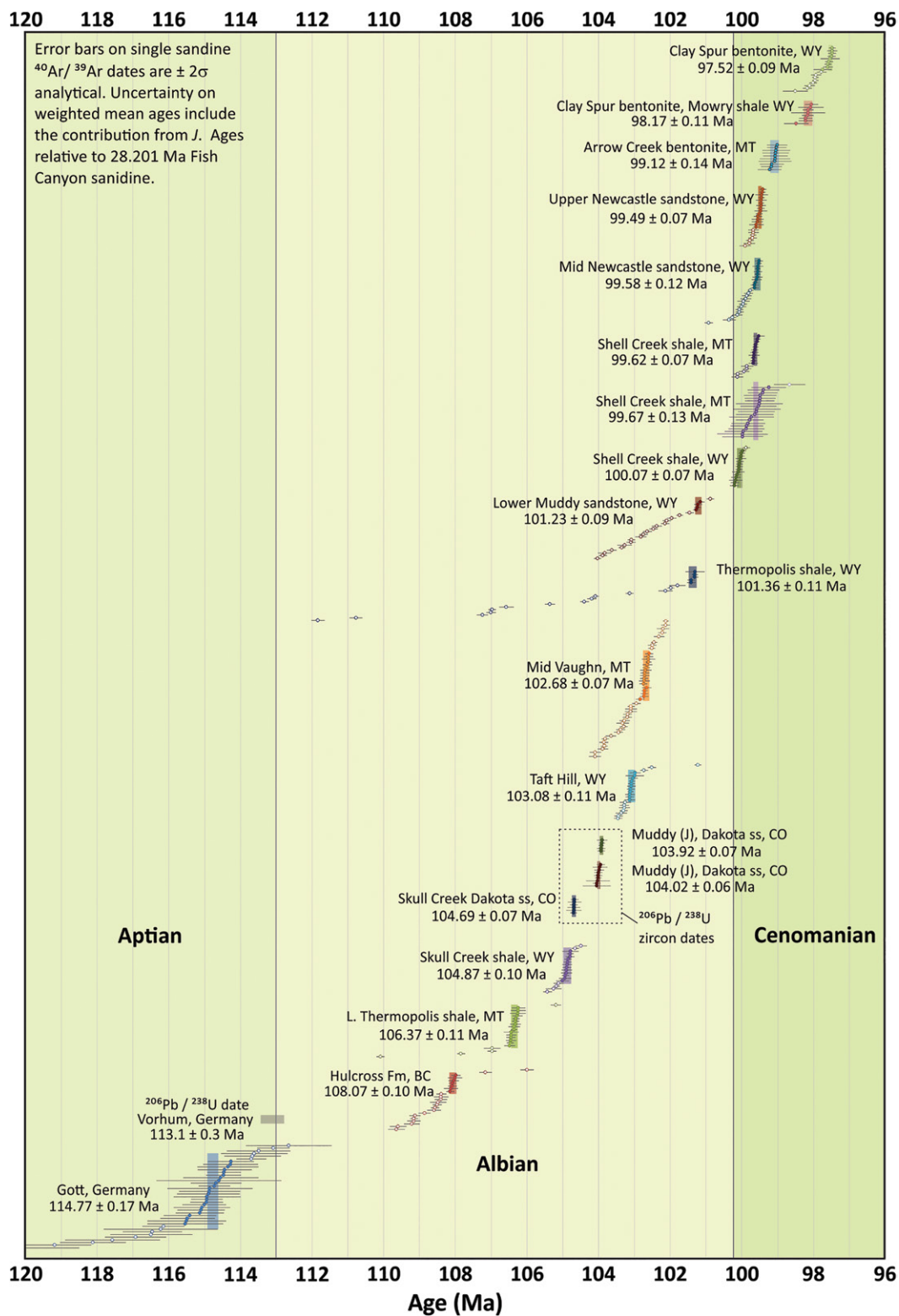


**Figure 4.** Rank order plot shows  $^{40}\text{Ar}/^{39}\text{Ar}$  dates from individual sanidine crystals in 14 bentonites from the Western Interior Basin, one from Gott, Germany, and one from the Hulcross Formation, British Columbia. Also shown are  $^{206}\text{Pb}/^{238}\text{U}$  zircon dates from three bentonites in the Dakota Sandstone in Colorado, USA, (dashed box) and from the Vorhum tuff, Germany (the latter from Selby et al., 2009). Filled symbols are dates used to calculate the weighted mean ages (vertical colored bars) at the 95% confidence level. Open symbols reflect dates that are not included in the weighted mean calculations. The Aptian-Albian and Albian-Cenomanian boundary ages are from Geologic Time Scale 2012 (Gradstein et al., 2012). Individual  $^{40}\text{Ar}/^{39}\text{Ar}$  dates relative to 28.201 Ma Fish Canyon sanidine are shown with  $\pm 2\sigma$  analytical uncertainties; the weighted mean age of each sample is shown with the analytical plus  $J$  value uncertainty. WY—Wyoming; MT—Montana; ss—sandstone; Fm—formation; BC—British Columbia.

Mowry Shale in the adjoining Wind River and Bighorn Basins, and possibly in the subsurface of the Powder River Basin (Slaughter and Early, 1965), is likely not the Clay Spur Bentonite of the Black Hills (Allison, 1988). Notwithstand-

ing, the 97.52 Ma age reported here for the bentonite at the top of Mowry Shale at Kaycee, along the southwestern border of the Powder River Basin (Fig. 2, Table 1), is our best estimate for the age of the top of the Mowry Shale,

a widely correlated horizon in the Powder River Basin of Wyoming.

The top of the Mowry or “Clay Spur” Bentonite has been widely used as a marker horizon in the Western Interior region (or basin) of the United

States and Canada (as the “Fish Scales” marker; Leckie et al., 1992) as an age for the boundary between the Upper and Lower Cretaceous (the top of the Albian stage). New age determinations demonstrate that the top of the Mowry Shale (sensu stricto) is early Cenomanian in age, confirming the interpretation of Reeside and Cobban (1960) and Cobban and Kennedy (1989) (and see also Amédro et al., 2002, and more recently Wilmsen et al., 2020) that the *Neogastropolites* fauna in Canada and the United States may be entirely of early Cenomanian age. If the “Fish Scale zone” in Canada is in any way correlative in age to the Mowry Shale, it must be presumed that it also is early Cenomanian (Fig. 5).

The next older ages discussed are from stratigraphic units at the base or just below the Mowry

Shale in Wyoming and Montana. (Fig. 3). The Arrow Creek Bentonite sample MT-09-06 was collected by Brad Singer and Brian Jicha from site #28 of Obradovich (1993) within the *Neogastropolites cornutus* zone (USGS Washington Mesozoic locality 24603; Walaszczyk and Cobban, 2016) of the Colorado Shale, immediately beneath beds correlated with the Mowry Shale (Reeside and Cobban, 1960, measured sections 13 and 14, p. 37–41, plate 1) in Judith Basin County, Montana. The Arrow Creek sanidine yields an age of  $99.12 \pm 0.10/0.14/0.21$  Ma (Table 1). It is shown (Fig. S3A) in the central Montana region near occurrences of Neogastropolid ammonites (Reeside and Cobban, 1960, annotated plate 1) and inoceramids (*Gnesioceramus mowriensis*) of Mowry age, and *Neogastropolites muelleri* and inoceramids of Shell Creek age (*Posidonioceramus nahwisi* zone; Walaszczyk and Cobban, 2016).

The Shell Creek Shale contains four dated bentonites including from the top of the unit in Montana (Arrow Creek Bentonite,  $99.12 \pm 0.10/0.14/0.21$  Ma; Fig. S3A), a 70 cm bentonite in the Wind River Basin south of Lander, Wyoming, that is  $99.62 \pm 0.04$  Ma (Figs. S6A–S6C), a bentonite near Greybull, Wyoming, that is  $99.67 \pm 0.11/0.13/0.20$  Ma (Figs. S3B, S9, S10, and S11; see footnote 1), and a bentonite in the Soap Creek Dome area of the Crow Indian Reservation just northeast of the Bighorn Basin in Wyoming and Montana (Fig. S5) that is  $100.07 \pm 0.03/0.07/0.17$  Ma. The latter bentonite age is probably the closest to the

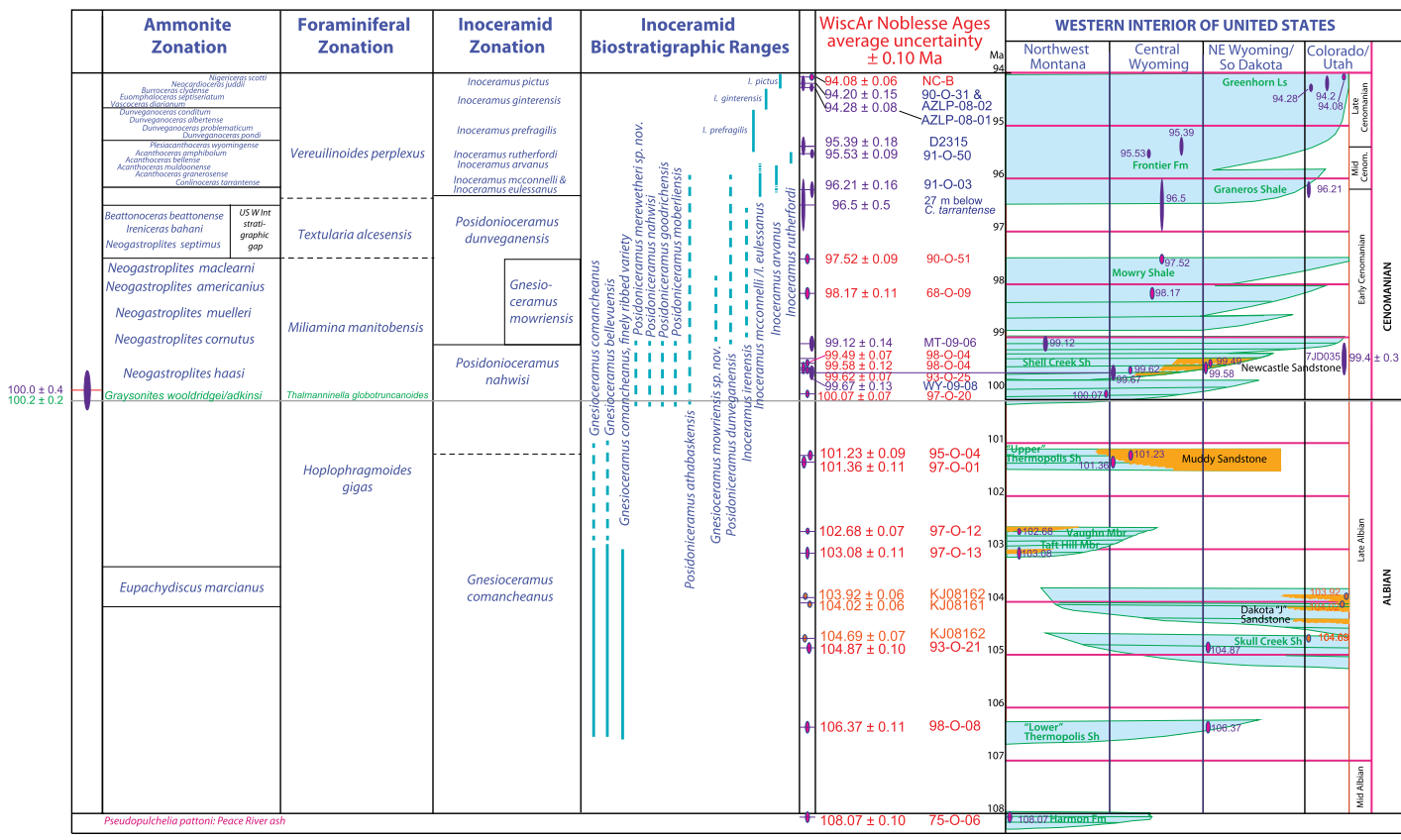


**Figure 5.** Biostratigraphic, chronostratigraphic, and schematic sequence stratigraphy of Albian to Cenomanian strata of the Western Interior Seaway in Wyoming, Montana, and Colorado, USA, is shown. Chronostratigraphic vertical scale is linear (Wheeler diagram), while sequence stratigraphic horizontal scale is geographic from NW (Canada, Montana) to SE (Colorado). The radioisotopic dates are discussed in the main text. Ages in violet are single-collector mass spectrometer ages from WiscAr Laboratory and John D. Obradovich both published (Obradovich, 1993; Oboh-Ikuenobe et al., 2008) and unpublished. Biostratigraphic zonation of inoceramids, ammonites, and foraminifera from Walaszczyk and Cobban (2016); they document the ammonites and foraminifera coeval with the U.S. Western Interior stratigraphic gap between the Mowry Shale and the Graneros Shale that are present in the Western Canada Sedimentary Basin. Planktonic foraminifera *Thalmanninella (Rotaliora) globotruncanoides* and ammonite *Graysonites woolridgei* from dated Albian–Cenomanian Boundary section in Hokkaido, Japan, by Obradovich et al. (2002); the age is recalibrated to 28.201 FCs. Estimation of the Albian–Cenomanian boundary age is based on first appearance datum of *Thalmanninella globotruncanoides* in Yezo Group in Hokkaido, which Obradovich dated at  $100.0 \pm 0.4$  Ma (recalibrated to 28.201 Ma FCs from a reported age of  $99.33 \pm 0.37$  Ma in Cobban et al., 2006). Mbr—member; Sh—shale; Fm—formation; Ls—limestone; US W Int—U.S. Western Interior.

Albian–Cenomanian boundary in the Western Interior Basin of North America. A subjacent sample re-collected by Cobban and Merewether (97-O-19) from a sand-rich interval disturbed by sandstone dikes and corresponding to the Muddy Sandstone was dated by Obradovich at  $100.65 \pm 0.39$  Ma (relative to 28.201 Ma FCs) but never published. It falls exactly in the gap between the oldest Shell Creek Shale age ( $100.07 \pm 0.03/0.07/0.17$  Ma) and the Muddy Sandstone age at Maverick Springs Dome of  $101.23 \pm 0.05/0.09/0.18$  Ma (Table 1).

Bentonites corresponding to the middle of the range of Shell Creek Shale ages (99.12–100.07 Ma) were dated from the Newcastle Sandstone in the northwestern Black Hills north of Devils Tower near Hulett, Crook County, Wyoming (Davis and Izett, 1962). The Noblesse ages are  $99.49 \pm 0.03/0.07/0.17$  Ma for the upper bentonite and  $99.58 \pm 0.03/0.12/0.19$  Ma for the middle bentonite (Fig. S4). Although these ages are statistically distinct by  $90 \pm 40$  ka if one considers only the internal analytical uncertainties, given the uncertainties of the *J* values, a difference in age cannot be confirmed. Notwithstanding, it is certain that the age of the Newcastle in the northwestern Black Hills is entirely early Cenomanian. The lowest of the three bentonites interfingering with the Newcastle Sandstone has not been dated using the WiscAr Noblesse but was determined by J.D. Obradovich at  $99.8 \pm 0.4$  Ma (personal communication, 2008), which is not distinguishable from the more precise Noblesse ages determined from middle and upper Newcastle (Table 1). This indicates that all of the clastic shoreface sandstones atop the Western Interior transgressional Dakota Sandstone interval on the eastern margin of the Powder River Basin are early Cenomanian and distinctly younger by ca. 1.6 Ma than the Muddy Sandstone in the Big-horn and Wind River Basins of central Wyoming (Fig. 3). The  $99.62 \pm 0.03/0.07/0.17$  Ma age from a single 70-cm-thick bentonite in the lower Shell Creek Shale that crops out just above the Muddy Sandstone in the Wind River Basin on U.S. Highway 287, south of Lander, Wyoming, is indistinguishable from the middle and upper Newcastle Sandstone ages given the uncertainties that include the *J* value. Thus, it constrains the early Cenomanian shoreface paleogeography of central and northeastern Wyoming at 99.6 Ma (Figs. 1 and 5).

Two new dates constrain deposition of the Muddy Sandstone in northern and central Wyoming, one from the top of this unit in the Wind River Basin and the other just below it in the Bighorn Basin. The sample from the Wind River Basin is from the northeast flank of Maverick Springs Dome 110 km northwest of the Shell

Creek age locality on the Wind River Reservation of the Eastern Shoshone and Northern Arapaho tribes, Fremont County, Wyoming (Fig. S6A). It is from the Muddy Sandstone area mapped by Dresser (1974) as one of the “two upper bentonites” from measured section locality 14, most likely the upper 4-foot bentonite (Fig. S6B). The four youngest of 46 sanidine crystals that span from 112 Ma to 101 Ma yield an age of  $101.23 \pm 0.05/0.09/0.18$  Ma (Table 1, Fig. 4). Given the profound inheritance of detrital crystals, this could be a minimum age, and the bentonite deposition may be younger. However, Obradovich obtained, but published only in an abstract, an age of  $101.32 \pm 0.25$  Ma (relative to 28.201 Ma FCs) from three separate irradiations of multi-grain (dozens) of hand-picked sanidine aliquots for this sample. The precise Noblesse age for a bentonite in the uppermost Thermopolis Shale just below the Muddy Sandstone at Greybull (Figs. S9, S10, and S11, see footnote 1; Eicher, 1960, 1962; Paull, 1962) yields an age of  $101.36 \pm 0.05/0.11/0.19$  Ma that is a maximum for the Muddy Sandstone in the northern Wind River and Bighorn Basins. Further insight into the age of the Muddy Sandstone comes from the northern Bighorn Mountain area in Montana, directly below the  $100.07 \pm 0.04$  Ma Shell Creek Shale Bentonite from Soap Creek Dome (Fig. S5). From sample 97-O-19 in the sand-rich horizon correlated with the Muddy Sandstone, at Soap Creek Dome on the Crow Indian Reservation, Montana, Obradovich obtained an age of  $100.65 \pm 0.20$  Ma (relative to 28.201 Ma) that was never published. It is 58 feet below the bentonite 97-O-20 from the Shell Creek Shale, which is dated here at  $100.07 \pm 0.03/0.07/0.17$  Ma. This sample illustrates the stratigraphic variability of the Muddy Sandstone between the Thermopolis Shale below and the Shell Creek Shale overlain by the Mowry Shale above (Fig. 3). This Muddy Sandstone horizon consists of discontinuous sandstone lenses injected by sandstone dikes and interlayered with a bentonite (Richards, 1955).

Stratigraphically, the next oldest ages are from two bentonites in the Blackleaf Formation in the Sweetgrass Arch geologic region, which is 17 km west of Great Falls, Cascade County, Montana. They are in the type section of the Blackleaf Formation described in Cobban et al. (1976). The  $102.68 \pm 0.03/0.07/0.18$  Ma Vaughn and  $103.08 \pm 0.03/0.11/0.20$  Ma Taft Hill members are significantly older than previous correlations to the Mowry Shale or Newcastle Sandstone (Cobban et al., 1976). These bentonites are part of an apparently continuous stratigraphic section that spans ca. 400 ka, passing disconformably from the marine, fossiliferous Taft Hill Member (Walaszczyk and Cobban, 2016)

up into zeolitic nonmarine Vaughn Member (Fig. S7). Stratigraphic units in this interval have not been documented in the north-central Wyoming composite section, and they do not correlate with nonmarine Frontier–Mowry age-equivalent sedimentary rocks called “Vaughn” in southwestern Montana (Zartman et al., 1995; Dyman et al., 2000) nor with strata in the Powder River Basin or Black Hills. The Taft Hill documents an extended period of marine sedimentation with multiple occurrences of *Gnesioceramus comancheanus*/*G. bellvuensis* (Fig. S7; Cobban et al., 1976; Walaszczyk and Cobban, 2016) that stratigraphically extend to levels possibly similar in age to the Dinosaur Ridge Dakota “J” Sandstone or Joli Fou Formation of Canada. It could stratigraphically correspond to the Crowsnest Volcanics interval in Canadian outcrops (Fig. 3), as suggested by recent but imprecise U-Pb ages of  $102.4 \pm 0.7$  Ma and  $103.8 \pm 1$  Ma on melanite garnet (Pana et al., 2018). More precise sanidine or zircon dates from the Crowsnest Volcanics are needed to bolster this correlation.

The oldest of the three U-Pb zircon ages from Dinosaur Ridge (Fig. S1; see footnote 1) is from the Skull Creek Shale beneath the upper Dakota Sandstone (Figs. S8 and S12; see footnote 1). Sample KJ08160 yields an age of  $104.69 \pm 0.05/0.07/0.13$  Ma and is beneath the Kassler Member (Waagé, 1961; MacKenzie, 1965; Weimer, 1996) and above the Plainview and Lytle Formations of the Dakota Sandstone. The sample was collected on the southwest side of the crest of the Alameda Avenue roadcut at Dinosaur Ridge and is marked by an exhibit and sign (Fig. S8). The second tuff sample, KJ08161, is stratigraphically higher in the overlying middle Kassler Member of the Dakota Sandstone and yields an age of  $104.02 \pm 0.04/0.06/0.13$  Ma that is ca. 670 ka younger than the Skull Creek Shale Bentonite age. A third sample, KJ08161, is from the north side of the roadcut in the slightly higher Kassler Member (Fig. 12B), and yields an age of  $103.92 \pm 0.04/0.06/0.13$  Ma (Table 1, Fig. 4). Although these three ages for the Dakota Sandstone are statistically distinct and agree with the local stratigraphy, they do not support correlations with the Muddy Sandstone of central Wyoming (102.23–103.32 Ma) nor with the Newcastle Sandstone of the Black Hills (99.6–99.5 Ma).

The Skull Creek age from Dinosaur Ridge of  $104.69 \pm 0.05/0.07/0.13$  Ma may correlate with the Skull Creek Shale in the northwestern Black Hills of Wyoming at  $104.87 \pm 0.04/0.10/0.19$  Ma, as these two ages may be only 180 ka apart given the internal uncertainties of the two methods or are indistinguishable from one another when the total uncertainties are considered. (Table 1). This Skull Creek sample is from the same area north

of Devils Tower, Wyoming, as the Newcastle Sandstone Bentonites that yield ages of 99.6–99.5 Ma. As they directly overlie the Skull Creek Shale, they provide evidence for an unconformity of 5 Ma. Obradovich determined the age of a sanidine from the lower part of the upper Dakota south of Colorado Springs at Deadman Canyon (Fig. S13; see footnote 1). This age, stratigraphically above the Purgatoire Formation (Cheyenne/Lytte-equivalent) and Glencairn Shale (Kiowa/Skull Creek-equivalent) Formations (Fig. S13; see footnote 1), was published in Oboh-Ikuenobe et al. (2008). It contains a measured section of the lower part of the upper Dakota, Dry Creek Canyon Member, with the analytical data in their Table 5 indicating an age of  $99.4 \pm 0.3$  Ma (relative to 28.201 Ma FCs) that we report in Table 1. This corresponds most closely to the ages of the Newcastle Sandstone from the Black Hills, but no one previously has suggested that the Dakota Sandstone along the Front Range could be 5 Ma younger than Skull Creek Shale at Dinosaur Ridge. Nor has there been a regional unconformity documented between the upper Dakota at Dinosaur Ridge and south of Colorado Springs. To further add to multiple stratigraphic hypotheses for the Dakota Sandstone in the Front Range of Colorado, Obradovich also determined an age for the lower of two bentonites of the “Skull Creek Shale” near Fort Collins at the outcrops north of Dixon Canyon Dam on Horsetooth Reservoir and obtained an age of  $100.6 \pm 0.2$  Ma (relative to 28.201 Ma FCs) that was never published. This age corresponds most closely to the Shell Creek Shale of Wyoming and Montana, between the Muddy Sandstone ages and the Newcastle Sandstone ages, but it is 4 Ma younger than the Skull Creek Shale in the Black Hills and at Dinosaur Ridge. These new data and observations confirm Bill Cobban’s observation that the chronostratigraphy of the Dakota Sandstone is complicated (“tricky”) due to unrecognized unconformities and the lack of Albian ammonites (e.g., Cobban and Reeside, 1952) in the Western Interior. In contrast, the Cenomanian facies of the Dakota Sandstone Group in New Mexico and Utah are already constrained by biostratigraphy (Cobban, 1977; Elder et al., 1994; Owen et al., 2007) and our earlier published ages (Meyers et al., 2012; Ma et al., 2014; Batenburg et al., 2016; Jones et al., 2020; Figs. S14 and S15; see footnote 1).

The three oldest Cretaceous bentonite ages reported here are from geographically dispersed localities (Wyoming, British Columbia, and Germany) and older discrete samples that are not constrained by other radioisotopically dated strata. These ages remain to be evaluated by future dating efforts and therefore have a lower degree of confidence than the ages discussed above.

The next age that can be stratigraphically related to the Cretaceous succession in central and northern Wyoming is from the lower part of the Thermopolis Shale. A sample collected 11.4 km north of Greybull, Big Horn County, Wyoming (Figs. S9, S10, and S11), in proximity to the type section for the Shell Creek Shale of Eicher (1960), yields an age of  $106.37 \pm 0.04/0.11/0.20$  Ma. The dated bentonite is from the “green marker bentonite” of Eicher (1960, 1962) in the lower part of the Thermopolis Shale between the “rusty beds” that are now generally considered to be part of the underlying and completely undated Cloverly Formation and the middle silty member of the Thermopolis Shale. Although it is in geographic proximity to the newly dated bentonite (sample 97-O-01; Table 1) in the upper member of the Thermopolis Shale that is stratigraphically just beneath the Muddy Sandstone north of Greybull, it is significantly older by 5 Ma. Thus, a significant unrecognized unconformity exists within the Thermopolis Shale. It also does not correlate with the age of the Skull Creek Shale previously described from the northwest border of the Black Hills in Crook County, Wyoming, being 1.5 Ma older.

The Peace River Ash is from the Hulcross Formation, 50 m below the top of the Hulcross Formation, from the Gates, which is 9.8 km northeast of Hudson Hope, British Columbia, Canada. Considered to be in the middle Albian *Pseudopuchellia pattoni* ammonite zone (Obradovich, 1993), the new age determined for this bentonite is  $108.07 \pm 0.05/0.10/0.20$  Ma based on sample 75-O-06 of Obradovich (1993; locality #31), consistent with the coeval ages of sanidine and zircon reported by Hathway et al. (2013). Recent investigations (Buckley and Plint, 2013) have placed the bentonite in the Harmon alloformation, corresponding to surface H4, at the boundary between allomembers HD and HE. It extends as a chronostratigraphic surface across a vast area of  $12,000 \text{ km}^2$  of the Peace River Plains in northeast British Columbia, Alberta, and the Northwest Territories.

Of the ages in Obradovich (1993), the oldest, from locality #32, contains a thin bentonite in the lower part of the Otto Gott clay pit, which is 21 km southeast of Hanover, Germany, within the upper Aptian *Parahoplites nutfieldiensis* ammonite zone. The sanidine crystals are very fine grained (<60  $\mu\text{m}$ ); thus, the individual dates are relatively imprecise. Notwithstanding, we obtain an age of  $114.77 \pm 0.15/0.17/0.26$  Ma (Fig. 4) that improves considerably upon the precision of the age of  $114.74 \pm 1.30$  Ma (recalibrated to 28.201 Ma FCs) reported by Obradovich (1993). Notably, the new age of  $114.77 \pm 0.15/0.17/0.26$  Ma from upper

Aptian strata is  $1.73 \pm 0.40$  Ma older than the U-Pb zircon age of the Aptian–Albian boundary interval tuff from the Schwickeleit Sub-Formation, Vöhrum, Germany, that is  $113.08 \pm 0.10/0.20/0.30$  Ma (Selby et al., 2009) when the full external uncertainties are considered. The Vöhrum tuff is only 65 cm above the first occurrence of *Leymeriella (Proleymeriella) schrammeni anterior*, and its radioisotopic age is used to support an age of 113 Ma for the Aptian–Albian boundary and a 12.45 Ma duration for the Aptian stage in GTS2012 (Fig. 4).

## CONCLUSIONS

Precise  $^{40}\text{Ar}/^{39}\text{Ar}$  sanidine and U-Pb zircon ages provide important constraints on the early evolution and sequence stratigraphy of the Western Interior Cretaceous Seaway. Sixteen new  $^{40}\text{Ar}/^{39}\text{Ar}$  ages and three U-Pb ages span the upper Albian and lower Cenomanian, thus bracketing the Albian–Cenomanian and, consequently, the Lower–Upper Cretaceous series boundary (Fig. 4). In the Western Interior, beneath the middle Cenomanian–mid Maastrichtian ammonite zonation (99.6–69.6 Ma) of Cobban et al. (2006), there are multiple unconformities and disconformities—definitely more than have been previously identified. A clear lesson from this first extensive set of high-precision radioisotopic dates from these strata is that correlations based on similarity of lithologies, without independent radioisotopic ages or detailed biostratigraphic constraints, can be problematic or invalid. Specifically, the Dakota “J” Sandstone (103.9–104.0 Ma) of the Denver Basin is not stratigraphically equivalent to the Muddy Sandstone of central Wyoming (101.2 Ma), which is not correlative with the Newcastle Sandstone (99.6–99.5 Ma) of the eastern Powder River Basin and Black Hills. The Skull Creek Shale of the Denver Basin (104.9 Ma) may be correlative with the Skull Creek Shale (104.7 Ma) of the Black Hills, but the overlying sandstones are not. The Skull Creek Shale in the Black Hills–Powder River Basin is not the same age as the lower Thermopolis Shale (106.4 Ma) of the Bighorn Basin. The lower Cenomanian Newcastle Sandstone broadly overlaps in age with part of the Shell Creek Shale (100–99.3 Ma) in central Wyoming, and these strata likely record the Albian–Cenomanian boundary. Overall, there is much more time missing in unconformities than has been previously recognized.

## ACKNOWLEDGMENTS

We are indebted forever to John Obradovich and Bill Cobban, who pioneered the marriage of radioisotopic dating and biostratigraphy and supported us

intellectually in many ways during the course of this effort, and to Sam Bowring for taking up their mantle in the form of the EarthTime initiative. Thanks to Sarah Siewert, Kevin McKinney, Jahan Ramezani, and Kirk Johnson for invaluable assistance in the field and laboratory. Thoughtful reviews by Jim Ogg and Matt Heizler are much appreciated and helped to improve this paper in many ways. This work was supported in part by National Science Foundation grant EAR-0959108.

## REFERENCES CITED

Amédro, F., Cobban, W.A., Breton, G., and Rogron, P., 2002, *Metengonoceras teigenense* Cobban et Kennedy, 1989: Une ammonite exotique d'origine Nord-américaine dans le Cénomanien inférieur de Basse-Normandie (France): Bulletin Trimestriel de la Société Géologique de Normandie et des Amis du Muséum du Havre, v. 87, p. 5–28.

Allison, E.L., 1988, Bentonite mining in the Black Hills region: Wyoming Geological Association 39th Field Conference Guidebook, p. 305–313.

Andersen, N.L., Jicha, B.R., Singer, B.S., and Hildreth, W., 2017, Incremental heating of Bishop Tuff sanidine reveals preeruptive radiogenic Ar and rapid remobilization from cold storage: Proceedings of the National Academy of Sciences of the United States of America, v. 114, no. 47, p. 12,407–12,412, <https://doi.org/10.1073/pnas.1709581114>.

Batenburg, S.J., De Vleeschouwer, D., Sprovieri, M., Hilgen, F.J., Gale, A.S., Singer, B.S., Koerber, C., Coccioni, R., Claeys, P., and Montanari, A., 2016, Orbital control on the timing of oceanic anoxia in the Late Cretaceous: Climate of the Past Discussions, v. 12, no. 10, <https://doi.org/10.5194/cp-12-1995-2016>.

Bowring, J.F., McLean, N.M., and Bowring, S.A., 2011, Engineering cyber infrastructure for U-Pb geochronology: Tripoli and U-Pb\_Redux: Geochemistry, Geophysics, Geosystems v. 12, no. 6, <https://doi.org/10.1029/2010GC003479>.

Buckley, R.A., and Plint, A.G., 2013, Allostratigraphy of the Peace River Formation (Albian) in north-western Alberta and adjacent British Columbia: Bulletin of Canadian Petroleum Geology, v. 61, no. 4, p. 295–330, <https://doi.org/10.2113/gscpgbull.61.4.295>.

Clyde, W.C., Ramezani, J., Johnson, K.R., Bowring, S.A., and Jones, M.M., 2016, Direct high-precision U-Pb geochronology of the end-Cretaceous extinction and calibration of Paleocene astronomical timescales: Earth and Planetary Science Letters, v. 452, p. 272–280, <https://doi.org/10.1016/j.epsl.2016.07.041>.

Cobban, W.A., 1977, Characteristic marine molluscan fossils from the Dakota Sandstone and intertongued Manscos Shale, west central New Mexico: U.S. Geological Survey Professional Paper 1009, 30 p., <https://doi.org/10.3133/pp1009>.

Cobban, W.A., 1993, Diversity and distribution of Late Cretaceous ammonites, Western Interior, United States, in Caldwell, W.G.E., and Kauffman, E.G., eds., Evolution of the Western Interior Basin: Geological Association of Canada Special Paper 39, p. 435–451.

Cobban, W.A., and Kennedy, W.J., 1989, The ammonite Metengonoceras Hyatt, 1903, from the Mowry Shale (Cretaceous) of Montana and Wyoming: U.S. Geological Survey Bulletin 1787, 30 p.

Cobban, W.A., and Reeside, J.B., Jr., 1952, Correlation of the Cretaceous formations of the Western Interior of the United States: Geological Society of America Bulletin, v. 63, p. 1011–1044, [https://doi.org/10.1130/0016-7606\(1952\)63\[1011:COTCFO\]2.0.CO;2](https://doi.org/10.1130/0016-7606(1952)63[1011:COTCFO]2.0.CO;2).

Cobban, W.A., Erdmann, C.E., Lemke, R.W., and Maughan, E.K., 1976, Type sections and stratigraphy of the Members of the Blackleaf and Marias River Formations (Cretaceous) of the Sweetgrass Arch, Montana: U.S. Geological Survey Professional Paper 974, 71 p., <https://doi.org/10.3133/pp974>.

Cobban, W.A., Walaszczyk, I., Obradovich, J.D., and McKinney, K.C., 2006, A USGS zonal table for the Upper Cretaceous Middle Cenomanian-Maastrichtian of the Western Interior of the United States based on ammonites, inoceramids, and radiometric ages: U.S. Geological Survey Open-File Report 2006-1250, 47 p., <https://doi.org/10.3133/ofr20061250>.

Darton, N.H., 1904, Comparison of the stratigraphy of the Black Hills, Bighorn Mountains, and Rocky Mountain Front Range: Geological Society of America Bulletin, v. 15, p. 379–448, <https://doi.org/10.1130/GSAB-15-379>.

Davis, R.E., and Izett, G.A., 1962, Geology and uranium deposits of the Strawberry Hill Quadrangle, Crook County, Wyoming: U.S. Geological Survey Bulletin 1127, 86 p.

Dolson, J.C., and Muller, D.S., 1994, Stratigraphic evolution of the Lower Cretaceous Dakota Group, Western Interior, USA, in Caputo, M.V., Peterson, J.A., and Franczyk, K.J., eds., Mesozoic Systems of the Rocky Mountain Region: Tulsa, Oklahoma, SEPM (Society for Sedimentary Geology), p. 441–456.

Dresser, H.W., 1974, Muddy Sandstone—Wind River Basin: Wyoming Geological Association: Earth Science Bulletin, v. 7, no. 1, p. 5–70.

Dyman, T.S., Porter, K.W., Tysdal, R.G., Cobban, W.A., and Obradovich, J.D., 2000, Late Albian Blackleaf and Thermopolis-Muddy Sequence in southwestern Montana and correlation with time-equivalent strata in west-central Montana, in Montana Geological Society 50th Anniversary Symposium, Volume I: Billings, Montana, Montana Geological Society, p. 65–81.

Eicher, D.L., 1960, Stratigraphy and Micropaleontology of the Thermopolis Shale: Peabody Museum of Natural History Yale University Bulletin 15, 145 p.

Eicher, D.L., 1962, Biostratigraphy of the Thermopolis, Muddy, and Shell Creek Formations: Wyoming Geological Association Guidebook, v. 17, p. 72–93.

Elder, W.P., Gustason, E.R., and Sageman, B.B., 1994, Correlation of basinal carbonate cycles to nearshore parasequences in the Late Cretaceous Greenhorn seaway, Western Interior USA: Geological Society of America Bulletin, v. 106, no. 7, p. 892–902, [https://doi.org/10.1130/0016-7606\(1994\)106<892:COBCT>2.3.CO;2](https://doi.org/10.1130/0016-7606(1994)106<892:COBCT>2.3.CO;2).

Fassett, J.E., 2014, San Juan Basin, in Rogers, J.P., Milne, J.J., Cumella, S.P., DuBois, D., and Lillis, P.G., eds., Oil and Gas Fields of Colorado: Denver, Colorado, Rocky Mountain Association of Geologists, p. 298–306.

Gale, A.S., Kennedy, W.J., Burnett, J.A., Caron, M., and Kidd, B.E., 1996, The Late Albian to Early Cenomanian succession at Mont Risou near Rosans (Drome, SE France): An integrated study (ammonites, inoceramids, planktonic foraminifera, nanofossils, oxygen and carbon isotopes): Cretaceous Research, v. 17, p. 515–606, <https://doi.org/10.1006/cres.1996.0032>.

Gale, A.S., Bown, P., Caron, M., Crampton, J., Crowhurst, S.J., Kennedy, W.J., Petrizzi, M.R., and Wray, D.S., 2011, The uppermost Middle and Upper Albian succession at the Col de Palluel, Hautes-Alpes, France: An integrated study (ammonites, inoceramid bivalves, planktonic foraminifera, nanofossils, geochemistry, stable oxygen and carbon isotopes, cyclostratigraphy): Cretaceous Research, v. 32, p. 59–130, <https://doi.org/10.1016/j.cretres.2010.10.004>.

Gerstenberger, H., and Haase, G., 1997, A highly effective emitter substance for mass spectrometric Pb isotope ratio determinations: Chemical Geology, v. 136, no. 3–4, p. 309–312, [https://doi.org/10.1016/S0009-2541\(96\)00033-2](https://doi.org/10.1016/S0009-2541(96)00033-2).

Gradstein, F.M., Ogg, J.G., Schmitz, M., and Ogg, G., Coordinators, 2004, The Geologic Time Scale: Amsterdam, The Netherlands, Elsevier, 648 p.

Gradstein, F.M., Ogg, J.G., Schmitz, M., and Ogg, G., eds., 2012, The Geologic Time Scale: Amsterdam, The Netherlands, Elsevier, 1176 p.

Gustason, E.R., 1988, Depositional and tectonic history of the Lower Cretaceous Muddy Sandstone, Lazy B field, Powder River Basin, Wyoming, in Diedrich, R.P., Dyka, M.A.K., and Miller, W.R., eds., Wyoming Geological Association 39th Annual Field Conference Guidebook: Eastern Powder River Basin—Black Hills, p. 129–146.

Hathaway, B., Dolby, G., McNeil, D.H., Kamo, S.L., Heizler, M.T., and Joyce, N., 2013, Revised stratigraphy, regional correlations and new bentonite radiometric ages for the Albian Loon River Formation, Fort St. John Group, northwestern Alberta: Bulletin of Canadian Petroleum Geology, v. 61, p. 331–358, <https://doi.org/10.2113/gscpgbull.61.4.331>.

Hicks, J.F., Obradovich, J.D., and Tauxe, L., 1999, Magnetostratigraphy, isotopic age calibration and intercontinental correlation of the Red Bird section of the Pierre Shale, Niobrara County, Wyoming, USA: Cretaceous Research, v. 20, p. 1–27, <https://doi.org/10.1006/cres.1998.0133>.

Hicks, J.F., Johnson, K.R., Obradovich, J.D., Tauxe, L., and Clark, D., 2002, Magnetostratigraphy and geochronology of the Hell Creek and basal Fort Union Formations of southwestern North Dakota and a recalibration of the age of the Cretaceous-Tertiary boundary, in Hartman, J.H., Johnson, K.R., and Nichols, D.J., eds., The Hell Creek Formation and the Cretaceous-Tertiary Boundary in the Northern Great Plains: Geological Society of America Special Paper 361, p. 35–55.

Higley, D.K., Cox, D.O., and Weimer, R.J., 2003, Petroleum system and Production characteristics of the Muddy (J) Sandstone (Lower Cretaceous) Wattenberg continuous gas field, Denver Basin, Colorado: The American Association of Petroleum Geologists Bulletin, v. 87, no. 1, p. 15–37.

Jaffey, A.H., Flynn, K.F., Glendenin, L.E., Bentley, W.T., and Essling, A.M., 1971, Precision measurement of half-lives and specific activities of  $^{235}\text{U}$  and  $^{238}\text{U}$ : Physical Review C, v. 4, no. 5, p. 1889, <https://doi.org/10.1103/PhysRevC.4.1889>.

Jicha, B.R., Singer, B.S., and Sobol, P., 2016, Re-evaluation of the ages of  $^{40}\text{Ar}/^{39}\text{Ar}$  sanidine standards and supereruptives in the western U.S. using a Noblesse multi-collector mass spectrometer: Chemical Geology, v. 431, p. 54–66, <https://doi.org/10.1016/j.chemgeo.2016.03.024>.

Jones, M.M., Sageman, B.B., Selby, D., Jicha, B.R., Singer, B.S., and Titus, A.L., 2020, Regional chronostratigraphic synthesis of the Cenomanian-Turonian Oceanic Anoxic Event 2 (OAE2) interval, Western Interior Basin (USA): New Re-Os chemostratigraphy and  $^{40}\text{Ar}/^{39}\text{Ar}$  geochronology: Geological Society of America Bulletin, v. 133, <https://doi.org/10.1130/B35594.1>.

Joo, Young Ji, and Sageman, B.B., 2014, Cenomanian to Campanian carbon isotope chemostratigraphy from the Western Interior Basin, U.S.A.: Journal of Sedimentary Research, v. 84, p. 529–542, <https://doi.org/10.2110/jsr.2014.38>.

Kauffman, E.G., Sageman, B.B., Kirkland, J.I., Elder, W.P., Harries, P.J., and Villamil, T., 1993, Molluscan biostratigraphy of the Cretaceous Western Interior Basin, North America, in Caldwell, W.G.E., and Kauffman, E.G., eds., Evolution of the Western Interior Basin: Geological Association of Canada Special Paper 39, p. 397–434.

Kennedy, W.J., and Gale, A.S., 2006, The Cenomanian Stage: Proceedings of the Geologists' Association, v. 117, p. 187–205.

Kennedy, W.J., Gale, A.S., Lees, J.A., and Caron, M., 2004, The Global Boundary Stratotype Section and Point (GSSP) for the base of the Cenomanian Stage, Mont Risou, Hautes-Alpes, France: Episodes, v. 27, no. 1, p. 21–32, <https://doi.org/10.18814/epiugs/2004/271/003>.

Knechtel, M.M., and Patterson, S.H., 1955, Bentonite deposits of the northern Black Hills District, Wyoming, Montana, and South Dakota: U.S. Geological Survey Miscellaneous Field Studies Map 36, scale 1:48,000.

Kuiper, K.F., Deino, A., Hilgen, F.J., Krijgsman, W., Renne, P.R., and Wijbrords, J.R., 2008, Synchronizing rock clocks of Earth history: Science, v. 320, p. 500–504, <https://doi.org/10.1126/science.1154339>.

Leckie, D.A., Singh, C., Bloch, J., Wilson, M., and Wall, J., 1992, An anoxic event at the Albian-Cenomanian boundary—The Fish Scale Marker Bed, northern Alberta, Canada: Palaeogeography, Palaeoclimatology, Palaeoecology, v. 92, p. 139–166, [https://doi.org/10.1003/0182\(92\)90139-V](https://doi.org/10.1003/0182(92)90139-V).

Lee, J.-Y., Marti, K., Severinghaus, J.P., Kawamura, K., Yoo, H.-S., Lee, J.B., and Kim, J.S., 2006, A redetermination of the isotopic abundance of atmospheric Ar: Geochimica et Cosmochimica Acta, v. 70, p. 4507–4512, <https://doi.org/10.1016/j.gca.2006.06.1563>.

Leslie, C.E., Peppe, D.J., Williamson, T.E., Heizler, M., Jackson, M., Atchley, S.C., Nordt, L., and Standhardt, B.,

2018, Revised age constraints for Late Cretaceous to early Paleocene terrestrial strata from the Dawson Creek section, Big Bend National Park, west Texas: Geological Society of America Bulletin, v. 130, p. 1143–1163, <https://doi.org/10.1130/B31785.1>.

Ma, C., Meyers, S.R., Sageman, B.B., Singer, B.S., and Jicha, B.R., 2014, Testing the astronomical time scale for oceanic anoxic event 2, and its extension into Cenomanian strata of the Western Interior Basin (USA): Geological Society of America Bulletin, v. 126, p. 974–989, <https://doi.org/10.1130/B30922.1>.

MacKenzie, D.B., 1965, Depositional environments of Muddy Sandstone, western Denver Basin, Colorado: The American Association of Petroleum Geologists Bulletin, v. 49, no. 2, p. 186–206.

Mattinson, J.M., 2005, Zircon U-Pb chemical abrasion (“CA-TIMS”) method: Combined annealing and multi-step partial dissolution analysis for improved precision and accuracy of zircon ages: Chemical Geology, v. 220, no. 1–2, p. 47–66, <https://doi.org/10.1016/j.chemgeo.2005.03.011>.

McLean, N.M., Bowring, J.F., and Bowring, S.A., 2011, An algorithm for U-Pb isotope dilution data reduction and uncertainty propagation: Geochemistry, Geophysics, Geosystems., v. 12, no. Q0AA18.

Mercer, C.M., and Hodges, K.V., 2016, ArAR—A software tool to promote the robust comparison of K-Ar and  $^{40}\text{Ar}/^{39}\text{Ar}$  dates published using different decay, isotopic, and monitor-age parameters: Chemical Geology, v. 440, p. 148–163, <https://doi.org/10.1016/j.chemgeo.2016.06.020>.

Meyers, S.R., Siewert, S.E., Singer, B.S., Sageman, B.B., Condon, D., Obradovich, J.D., Jicha, B.R., and Sawyer, D.A., 2012, Intercalibration of radioisotopic and astrochronologic time scales for the Cenomanian/Turonian boundary interval, Western Interior Basin, USA: Geology, v. 40, p. 7–10, <https://doi.org/10.1130/G32261.1>.

Min, K., Mundil, R., Renne, P.R., and Ludwig, K.R., 2000, A test for systematic errors in  $^{40}\text{Ar}/^{39}\text{Ar}$  geochronology through comparison with U/Pb analysis of 1.1-Ga rhyolite: Geochimica et Cosmochimica Acta, v. 64, p. 73–98, [https://doi.org/10.1016/S0016-7037\(99\)00204-5](https://doi.org/10.1016/S0016-7037(99)00204-5).

Mossop, G.D., and Shetsen, I., comp., 1994, Geologic atlas of the Western Canada Sedimentary Basin: Canadian Society of Petroleum Geologists and Alberta Research Council, <http://ags.aer.ca/reports/atlas-of-the-western-canada-sedimentary-basin.htm> (accessed September 2020).

Oboh-Ikuenobe, F., Holbrook, J.M., Scott, R.W., Akins, S.L., Evetts, M.J., Benson, D.G., and Pratt, L.M., 2008, Anatomy of Epicontinental Flooding: Late Albian–Early Cenomanian of the Southern US Western Interior Basin: Geological Association of Canada Special Paper 48, p. 201–227.

Obradovich, J.D., 1993, A Cretaceous Time Scale, in Caldwell, W.G.E., and Kauffman, E.G., eds., Evolution of the Western Interior Basin: Geological Association of Canada, Special Paper 39, p. 379–396.

Obradovich, J.D., and Cobban, W.A., 1975, A time-scale for the Late Cretaceous of the Western Interior of North America, in Caldwell, W.G.E., ed., The Cretaceous System in the Western Interior of North America: Geological Association of Canada Special Paper 13, p. 31–45.

Obradovich, J.D., Matsumoto, T., Nishida, T., and Inoue, Y., 2002, Integrated biostratigraphic and radiometric study on the lower Cenomanian (Cretaceous) of Hokkaido, Japan: Proceedings of the Japan Academy, Series B, Physical and Biological Sciences, v. 78, no. 6, p. 149–153, <https://doi.org/10.2183/pjab.78.149>.

Ogg, J.G., and Hinnoo, L.A., 2012, Cretaceous, in Gradstein, F.M., Ogg, J.G., Schmitz, M., and Ogg, G., eds., The Geologic Time Scale 2012: Amsterdam, The Netherlands, Elsevier, p. 793–853, <https://doi.org/10.1016/B978-0-444-59425-9.00027-5>.

Owen, D.E., Siemers, C.T., and Owen, D.E., Jr., 2007, Dakota and adjacent lower Mancos Stratigraphy (Cretaceous and Jurassic) in the Holy Ghost Spring Quadrangle, Land of Pinchouts Jemez and Zia Indian Reservations, New Mexico, in Kues, B.S., Kelley, S.A., and Lueth, V.W., eds., Geology of the Jemez Region II: New Mexico Geological Society Guidebook, v. 58, p. 188–194.

Pana, D.I., Rukhlov, A.S., Hearman, L.M., and Hamilton, M., 2018, Geochronology of selected igneous rocks in the Alberta Rocky Mountains, with an overview of the age constraints on the host formations: Alberta Energy Regulator/Alberta Geological Survey Open-File Report 2018-03, 67 p.

Paull, R.A., 1962, Depositional history of the Muddy Sandstone, Big Horn Basin, Wyoming: Wyoming Geological Association Symposium on Early Cretaceous Rocks of Wyoming and Adjacent Areas; 17th Annual Field Conference Guidebook, p. 102–117.

Petrizzi, M.R., Caron, M., and Premoli Silva, I., 2015, Remarks on the identification of the Albian/Cenomanian boundary and taxonomic clarification of the planktonic foraminifera index species *globotruncanoides, brotzeni* and *tehamaensis*: Geological Magazine, v. 152, p. 521–536, <https://doi.org/10.1017/S0016756814000478>.

Plint, A.G., Krawetz, J.R., Buckley, R.A., Vannelli, K.M., and Walaszczyk, I., 2018, Tectonic, eustatic and climatic controls on marginal-marine sedimentation across a flexural depocentre: Paddy Member of Peace River Formation (Late Albian): Western Canada Foreland Basin: The Depositional Record, v. 4, p. 4–58, <https://doi.org/10.1002/dep2.37>.

Ramezani, J., Schmitz, M., Davydov, V., Bowring, S., Snyder, W., and Northrup, C., 2007, High-precision U-Pb zircon age constraints on the Carboniferous–Permian boundary in the southern Urals stratotype: Earth and Planetary Science Letters, v. 256, p. 244–257, <https://doi.org/10.1016/j.epsl.2007.01.032>.

Reeside, J.B., Jr., and Cobban, W.A., 1960, Studies of the Mowry Shale and contemporary formations in the United States and Canada: U.S. Geological Survey Professional Paper 355, 237 p., <https://doi.org/10.3133/pp355>.

Renne, P.R., Deino, A.L., Hilgen, F.J., Kuiper, K.F., Mark, D.F., Mitchell, W.S., Morgan, L.E., Mundil, R., and Smit, J., 2013, Time scales of critical events around the Cretaceous–Paleogene boundary: Science, v. 339, p. 684–687, <https://doi.org/10.1126/science.1230492>.

Richards, P.W., 1955, Geology of the Bighorn Canyon–Hardin Area, Montana and Wyoming: U.S. Geological Survey Bulletin 1026, 93 p.

Robinson, C.S., Mapel, W.J., and Bergendahl, M.H., 1964, Stratigraphy and structure of the northern and western flanks of the Black Hills uplift, Wyoming, Montana, and South Dakota: U.S. Geological Survey Professional Paper 404, 134 p., <https://doi.org/10.3133/pp404>.

Roca, X., Rylaardsma, J.R., Zhang, H., Varban, B.L., Sisulak, C.F., Bastedd, K., and Plint, A.G., 2008, An allostratigraphic correlation of the Lower Colorado Group (Albian) and equivalent strata in Alberta and British Columbia, and Cenomanian rocks of the Upper Colorado Group in southern Alberta: Bulletin of Canadian Petroleum Geology, v. 56, no. 4, p. 259–299, <https://doi.org/10.2113/gscpbull.56.4.259>.

Sageman, B.B., Singer, B.S., Meyers, S.R., Siewert, S.R., Walaszczyk, I., Condon, D.J., Jicha, B.R., Obradovich, J.D., and Sawyer, D.A., 2014, Integrating  $^{40}\text{Ar}/^{39}\text{Ar}$ , U-Pb, and astronomical clocks in the Cretaceous Niobrara Formation, Western Interior Basin, USA: Geological Society of America Bulletin, v. 126, p. 956–973, <https://doi.org/10.1130/B30299.1>.

Schaen, A.J., Jicha, B.R., Hodges, K.V., Vermeesch, P., Stelten, M.E., Mercer, C.M., Phillips, D., Rivera, T.A., Jourdan, F., Matchan, E.L., Hemming, S.R., Morgan, L.E., Kelley, S.P., Cassata, W.S., Heizler, M.T., Vasconcelos, P.M., Benowitz, J.A., Koppers, A.A.P., Mark, D.F., Niespolo, E.M., Sprain, C.J., Hames, W.E., Kuiper, K.F., Turrin, B.D., Renne, P.R., Ross, J., Nomade, S., Guillou, H., Webb, L.E., Cohen, B.A., Calvert, A.T., Joyce, N., Ganerød, M., Wijbrans, J., Ishizuka, O., He, H., Ramirez, A., Pfänder, J.A., Lopez-Martinez, M., Qiu, H., and Singer, B.S., 2020, Interpreting and reporting  $^{40}\text{Ar}/^{39}\text{Ar}$  geochronologic data: Geological Society of America Bulletin, <https://doi.org/10.1130/B35560.1>.

Schmitz, M.D., 2012, Radiogenic isotope geochronology, in Gradstein, F.M., Ogg, J.G., Schmitz, M., and Ogg, G., eds., The Geologic Time Scale 2012: Amsterdam, The Netherlands, Elsevier, p. 115–126, <https://doi.org/10.1016/B978-0-444-59425-9.00006-8>.

Scott, R.W., Oboh-Ikuenobe, F.E., Benson, D.G., Jr., Holbrook, J.M., and Alnahwi, A., 2018, Cenomanian–Turonian flooding cycles: U.S. Gulf Coast and Western Interior: Cretaceous Research, v. 89, p. 191–210, <https://doi.org/10.1016/j.cretres.2018.03.027>.

Selby, D., Mutterlose, J., and Condon, D.J., 2009, U/Pb and Re/Os geochronology of the Aptian/Albian and Cenomanian/Turonian stage boundaries: Implications for timescale calibration, osmium isotope seawater composition and Re-Os systematics in organic-rich sediments: Chemical Geology, v. 265, no. 3–4, p. 394–409, <https://doi.org/10.1016/j.chemgeo.2009.05.005>.

Slaughter, M., and Early, J.W., 1965, Mineralogy and Geological Significance of the Mowry Bentonites, Wyoming: Geological Society of America Special Paper 83, 116 p.

Sprain, C.J., Renne, P.R., Clemens, W.A., and Wilson, G.P., 2018, Calibration of Chron C29r: New high-precision geochronologic and paleomagnetic constraints from the Hell Creek Region, Montana: Geological Society of America Bulletin, v. 130, p. 1615–1644, <https://doi.org/10.1130/B31890.1>.

Thorson, T., 1976, Bentonite mining near Kaycee, Wyoming, in Laudon, R.B., Curry III, W.H., and Runge, J.S., eds., Geology and Energy Resources of the Powder River: Wyoming Geological Association 28th Field Conference Guidebook, p. 253–256.

Waagé, K.M., 1961, Stratigraphy and Refractory Clayrocks of the Dakota Group along the Northern Front Range, Colorado: U.S. Geological Survey Bulletin 1102, 154 p.

Walaszczyk, I., and Cobban, W.A., 2016, Inoceramid bivalves and biostratigraphy of the upper Albian and lower Cenomanian of the United States Western Interior Basin: Cretaceous Research, v. 59, p. 30–68, <https://doi.org/10.1016/j.cretres.2015.10.019>.

Weimer, R.J., 1984, Relation of unconformities, tectonics, and sea level changes, Cretaceous of Western Interior, U.S.A., in Schlee, J.S., ed., Interregional Unconformities and Hydrocarbon Accumulations: American Association of Petroleum Geologists Memoir 36, p. 7–35.

Weimer, R.J., 1996, Guide to Petroleum Geology and Laramide Orogeny, Denver Basin and Front Range: Colorado Geological Survey Bulletin, v. 51, 127 p.

Weimer, R.J., Sonnenberg, S.A., Davis, T.L., and Berryman, W.M., 1998, Stratigraphic and structural compartmentalization in the J and D Sandstones, central Denver Basin, Colorado, in Slatt, R.M., ed., Compartmentalized Reservoirs: Rocky Mountain Association of Geologists Special Publication, p. 1–27.

Wilmsen, M., Schumacher, D., and Niebuhr, B., 2020, The Early Cenomanian *crippsi* event at Lüneburg (Germany): Palaeontological and stratigraphical significance of a widespread Late Cretaceous bioevent: Palaeobiodiversity and Palaeoenvironments, in press.

Zartman, R.E., Dyman, T.S., Tysdal, R.G., and Pearson, R.C., 1995, U-Pb ages of volcanogenic zircon from porcellanite beds in the Vaughn Member of the Mid-Cretaceous Blackleaf Formation, southwest Montana, in Shorter Contributions to the Stratigraphy and Geochronology of Upper Cretaceous Rocks in the Western Interior of the United States: U.S. Geological Survey Bulletin, v. 2113-B, p. B1–B16.

SCIENCE EDITOR: ROB STRACHAN

ASSOCIATE EDITOR: XIXI ZHAO

MANUSCRIPT RECEIVED 15 JUNE 2020

REVISED MANUSCRIPT RECEIVED 15 SEPTEMBER 2020

MANUSCRIPT ACCEPTED 30 SEPTEMBER 2020

Printed in the USA